Photoluminescent Layered Lanthanide-Organic Framework Based on a Novel Trifluorotriphosphonate Organic Linker

Sérgio M. F. Vilela,[a,b] José A. Fernandes,[a] Duarte Ananias,[a] Luís D. Carlos,[c] João Rocha,[a] João P. C. Tomé,[b] Filipe A. Almeida Paz[a,*]

A contribution from

[a] *Department of Chemistry, CICECO, University of Aveiro, 3810-193 Aveiro, Portugal*

[b] *Department of Chemistry, QOPNA, University of Aveiro, 3810-193 Aveiro, Portugal*

[c] *Department of Physics, CICECO, University of Aveiro, 3810-193 Aveiro, Portugal*

Electronic Supporting Information

* *To whom correspondence should be addressed:*
Filipe A. Almeida Paz
Department of Chemistry, CICECO
University of Aveiro
3810-193 Aveiro
Portugal

E-mail: filipe.paz@ua.pt
FAX: (+351) 234 401470
Telephone: (+351) 234 401418

Table of Contents

1. Characterization of the organic molecules

1.1. NMR spectroscopy and mass spectrometry

1.1.1. 1,3,5-Tris(chloromethyl)-2,4,6-trifluorobenzene (L^1)

^{1}H NMR S3

^{13}C NMR S4

^{19}F NMR S5

1.1.2. Hexaethyl((2,4,6-trifluorobenzene-1,3,5-triyl)tris(methylene))tris(phosphonate) (L^2)

^{1}H NMR S6

^{13}C NMR S7

^{19}F NMR S8

Mass spectrum S9

1.1.3. ((2,4,6-Trifluorobenzene-1,3,5-triyl)tris(methylene))triphosphonic acid (H_6tftp)

^{1}H NMR S10

^{13}C NMR S11

^{19}F NMR S12

^{31}P NMR S13

Mass spectrum S14

1.2. Crystal structures

1.2.1. Crystallographic details S15

1.2.2. 1,3,5-Tris(chloromethyl)-2,4,6-trifluorobenzene (L^1) S17

1.2.3. Hexaethyl((2,4,6-trifluorobenzene-1,3,5-triyl)tris(methylene))tris-(phosphonate) (L^2) S18

1.2.4. ((2,4,6-Trifluorobenzene-1,3,5-triyl)tris(methylene))triphosphonic acid (H_6tftp) .. S19

2. Electron Microscopy Studies (EDS Mapping) and Powder X-ray Diffraction

2.1. [($La_{0.95}Eu_{0.05}$)(H_3tftp)(H_2O)] (2) S20

2.2. [($La_{0.95}Tb_{0.05}$)(H_3tftp)(H_2O)] (3) S21

2.3. [($La_{0.94}Eu_{0.03}Tb_{0.03}$)($H_3$tftp)($H_2O$)] (4) S22

3. Additional crystallographic representations: [La(H_3tftp)(H_2O)] S24

4. Solid-State NMR: [La(H_3tftp)(H_2O)] S25

5. FT-IR Spectroscopy S26

6. Thermogravimetry S27

7. Photoluminescence S28

8. References S34

1. Characterization of the organic molecules

1.1. NMR spectroscopy and mass spectrometry

1.1.1. 1,3,5-Tris(chloromethyl)-2,4,6-trifluorobenzene (*L*[1])

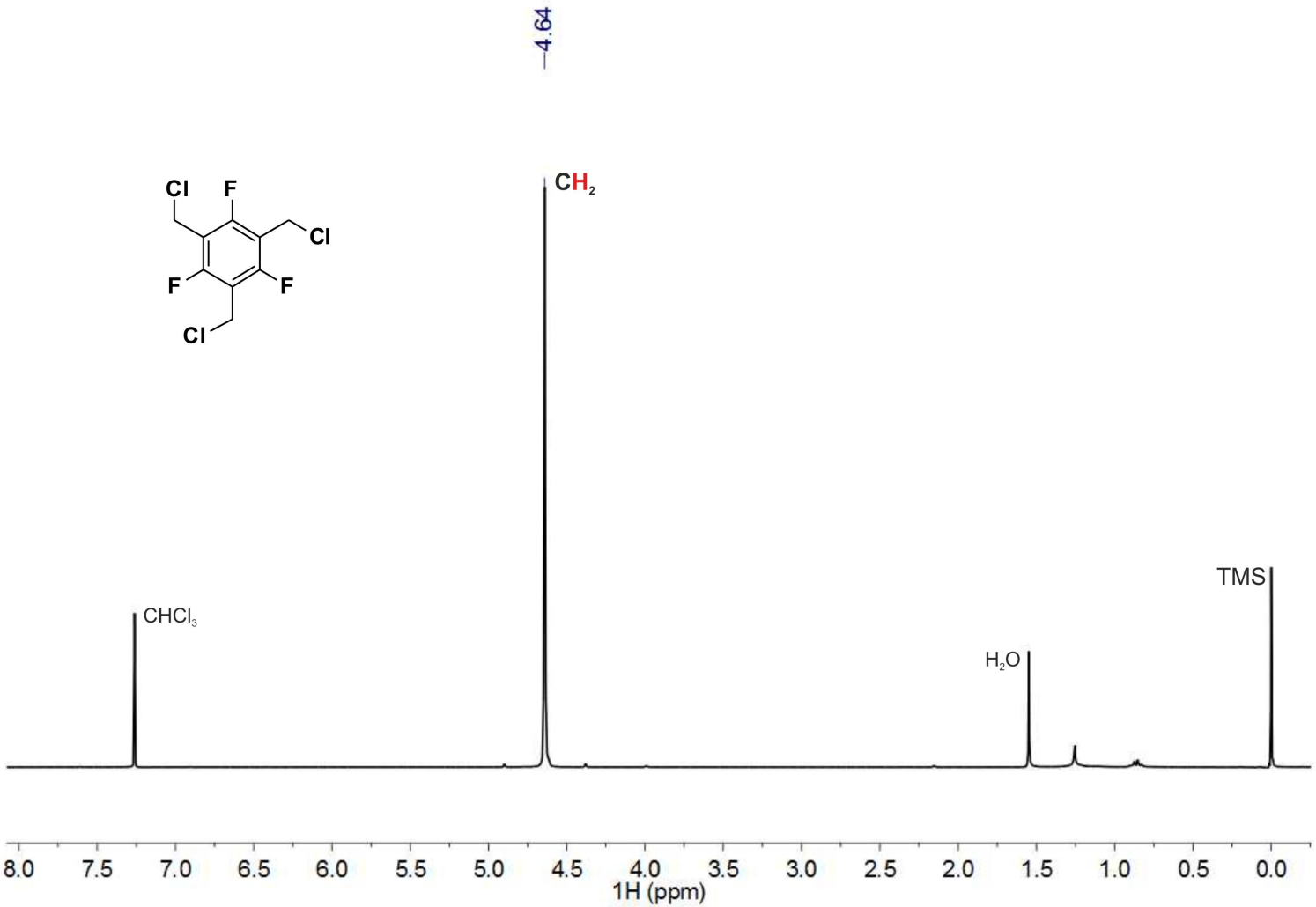

Fig. S1 ^{1}H NMR spectrum of the intermediate molecule 1,3,5-tris(chloromethyl)-2,4,6-trifluorobenzene in $CDCl_3$.

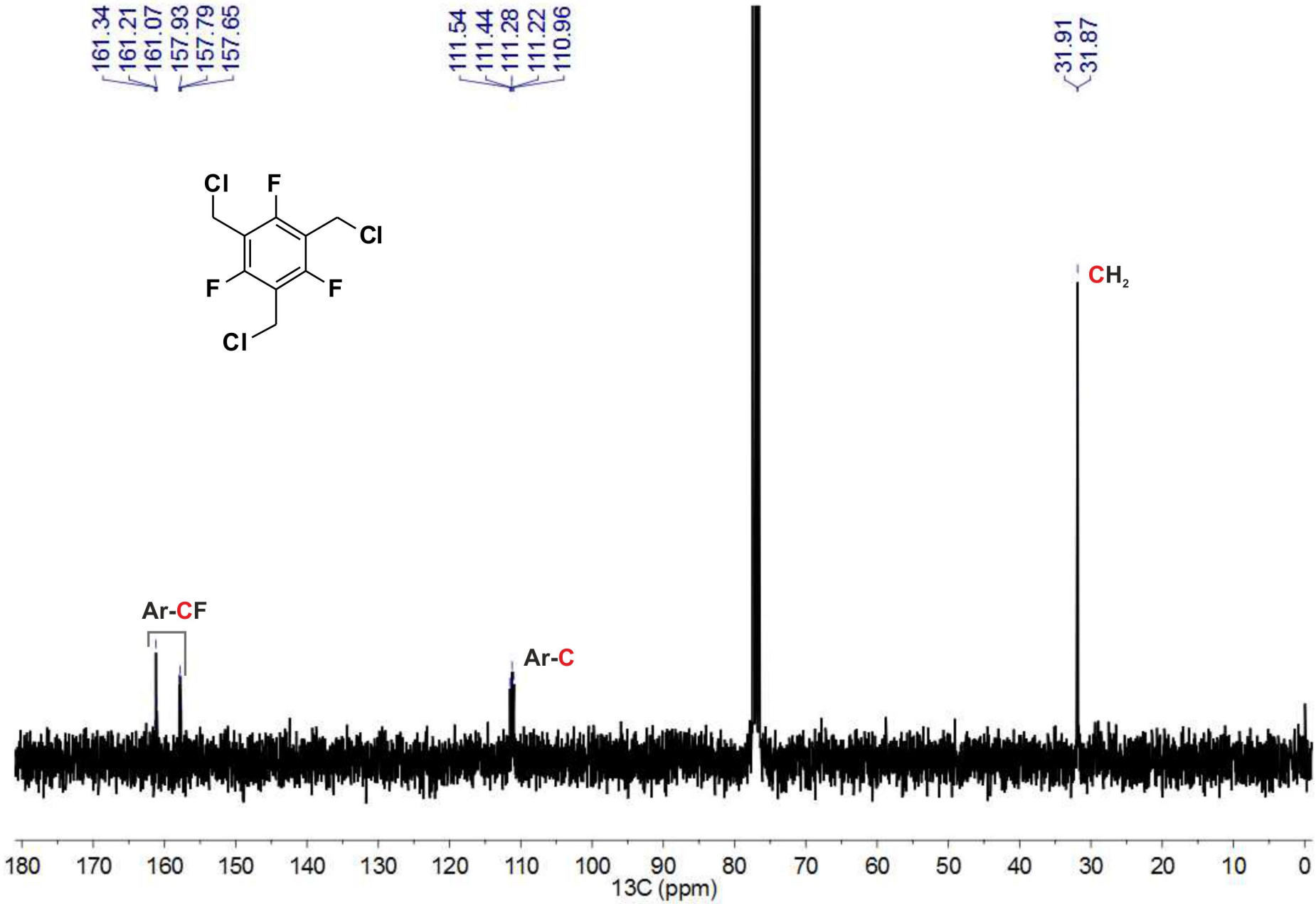

Fig. S2 ^{13}C NMR spectrum of the intermediate molecule 1,3,5-tris(chloromethyl)-2,4,6-trifluorobenzene in $CDCl_3$.

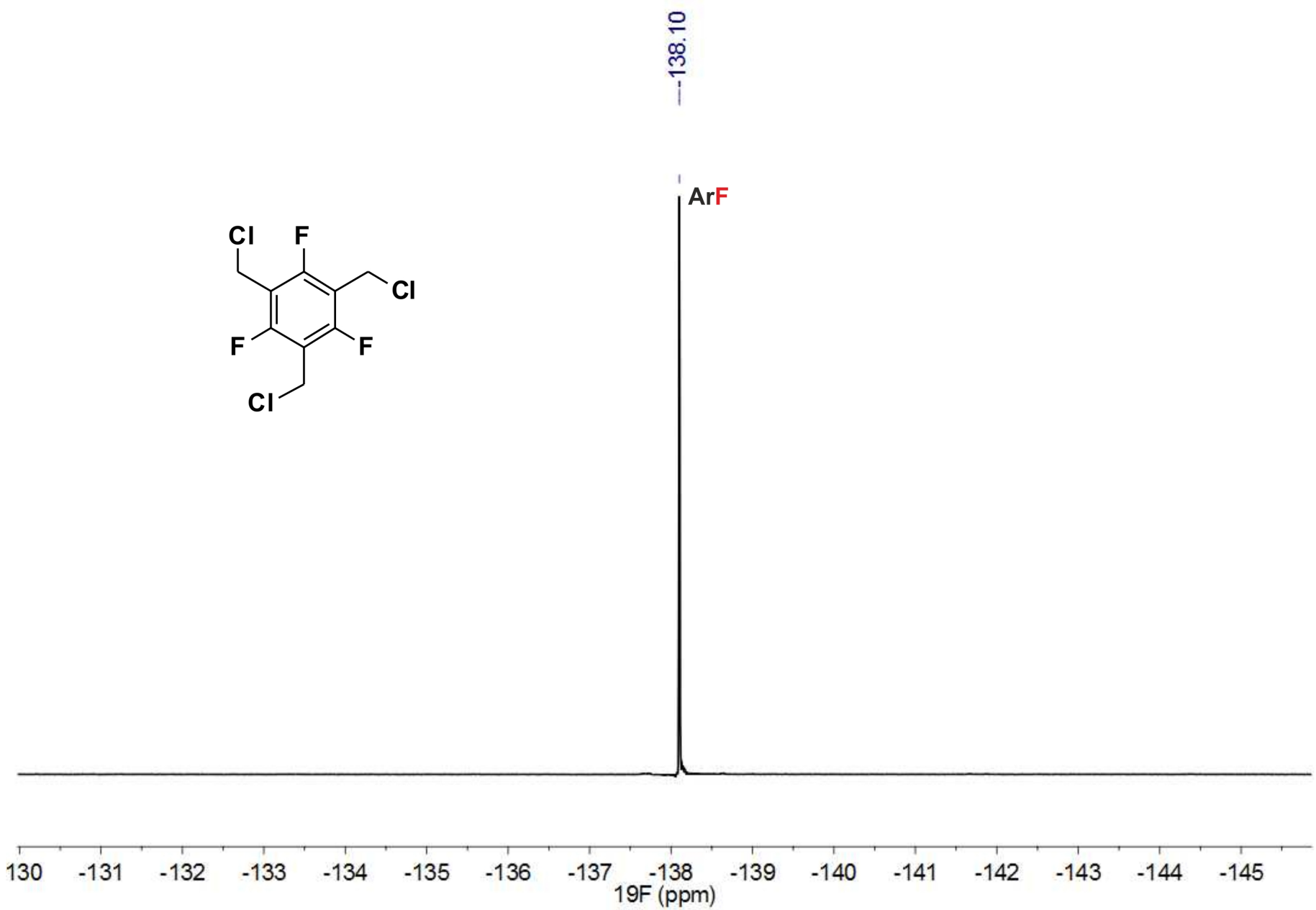

Fig. S3 ^{19}F NMR spectrum of the intermediate molecule 1,3,5-tris(chloromethyl)-2,4,6-trifluorobenzene in $CDCl_3$.

1.1.2. Hexaethyl((2,4,6-trifluorobenzene-1,3,5-triyl)tris(methylene))tris(phosphonate) (L^2)

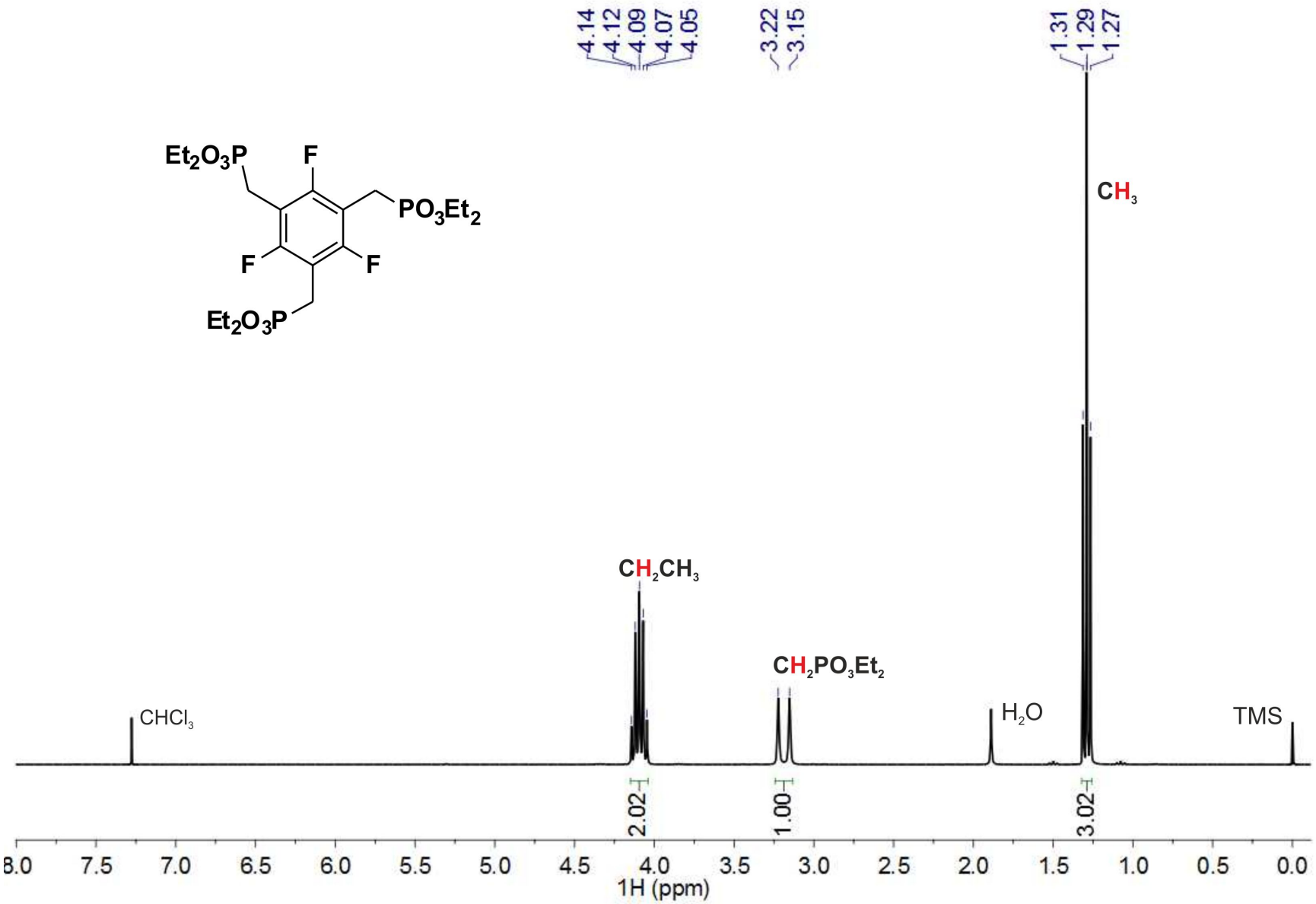

Fig. S4 ^{1}H NMR spectrum of the intermediate molecule hexaethyl((2,4,6-trifluorobenzene-1,3,5-triyl)tris(methylene))tris(phosphonate) in $CDCl_3$.

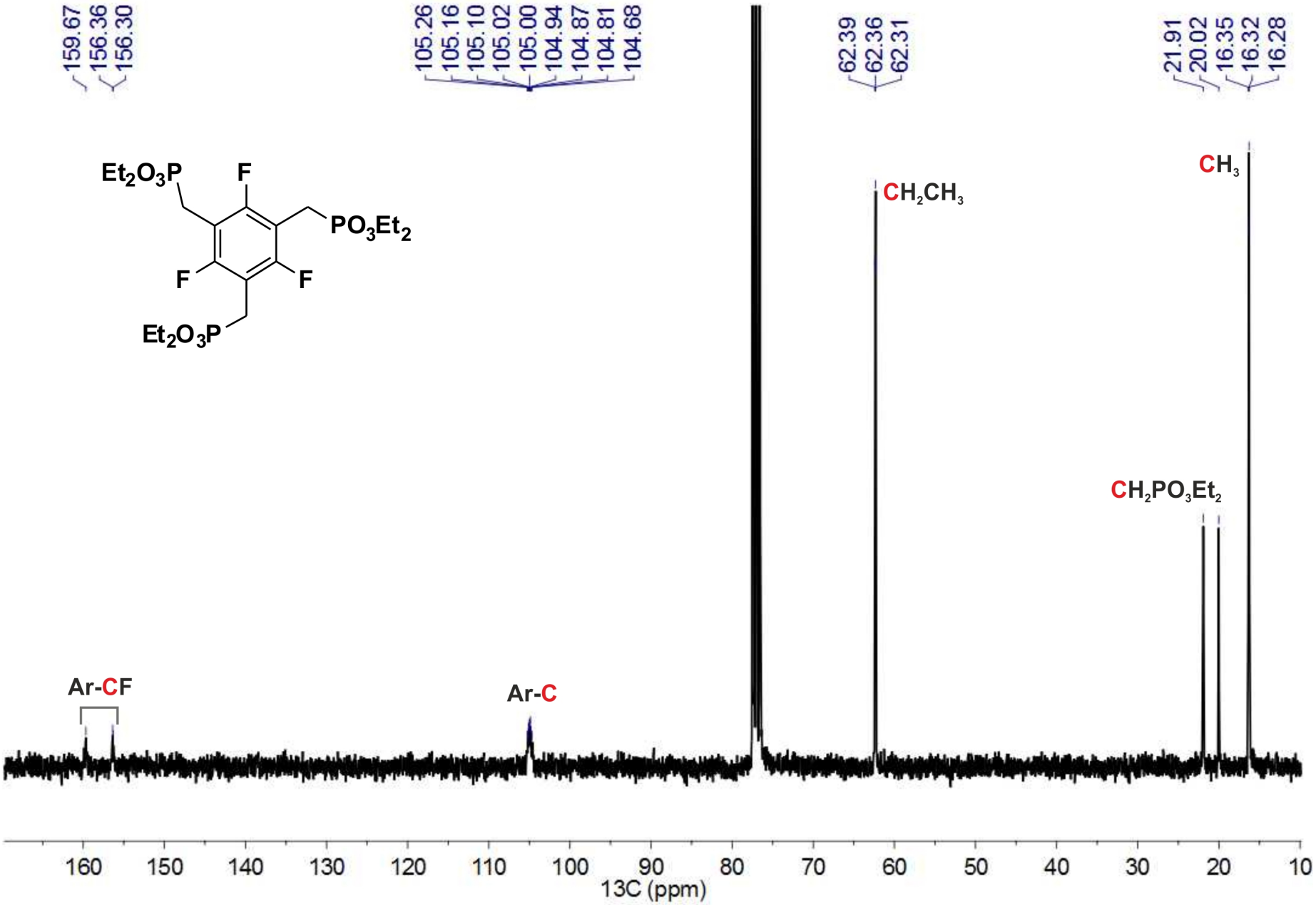

Fig. S5 ^{13}C NMR spectrum of the intermediate molecule hexaethyl((2,4,6-trifluorobenzene-1,3,5-triyl)tris(methylene))tris(phosphonate) in $CDCl_3$.

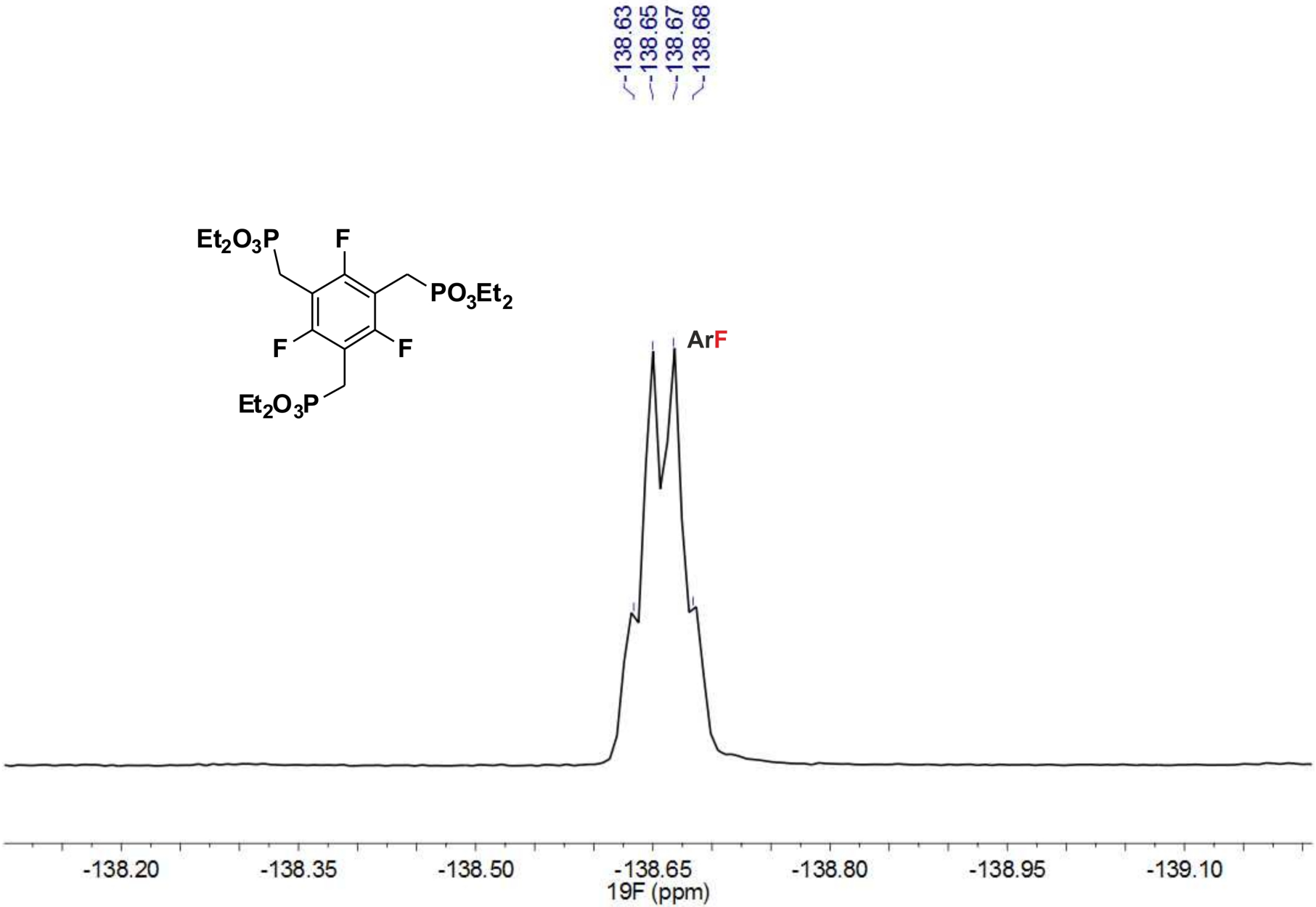

Fig. S6 ^{19}F NMR spectrum of the intermediate molecule hexaethyl((2,4,6-trifluorobenzene-1,3,5-triyl)tris(methylene))tris(phosphonate) in $CDCl_3$.

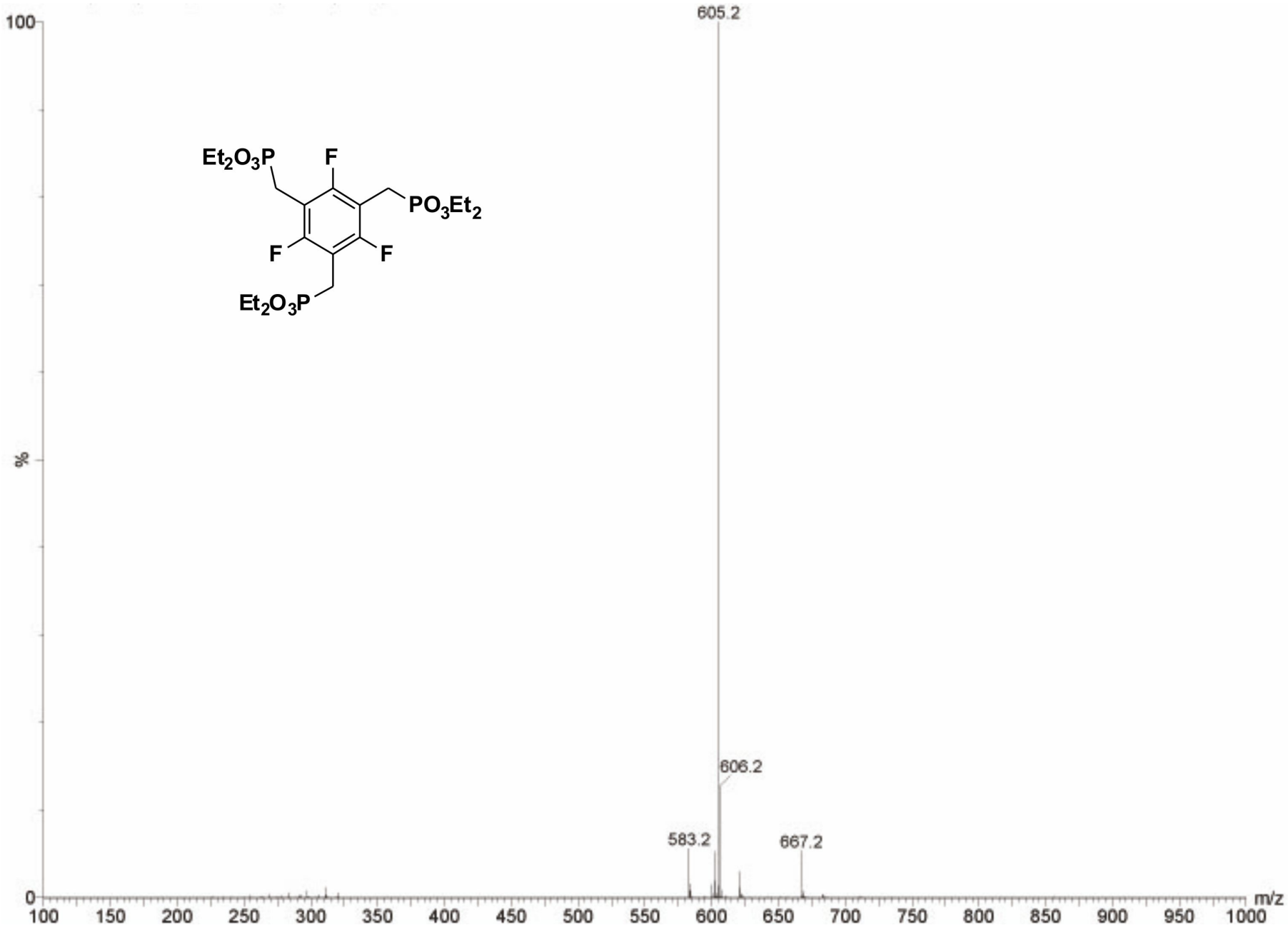

Fig. S7 Mass spectrum of the intermediate molecule hexaethyl((2,4,6-trifluorobenzene-1,3,5-triyl)tris(methylene))tris(phosphonate).

1.1.3. ((2,4,6-Trifluorobenzene-1,3,5-triyl)tris(methylene))triphosphonic acid (H_6tftp)

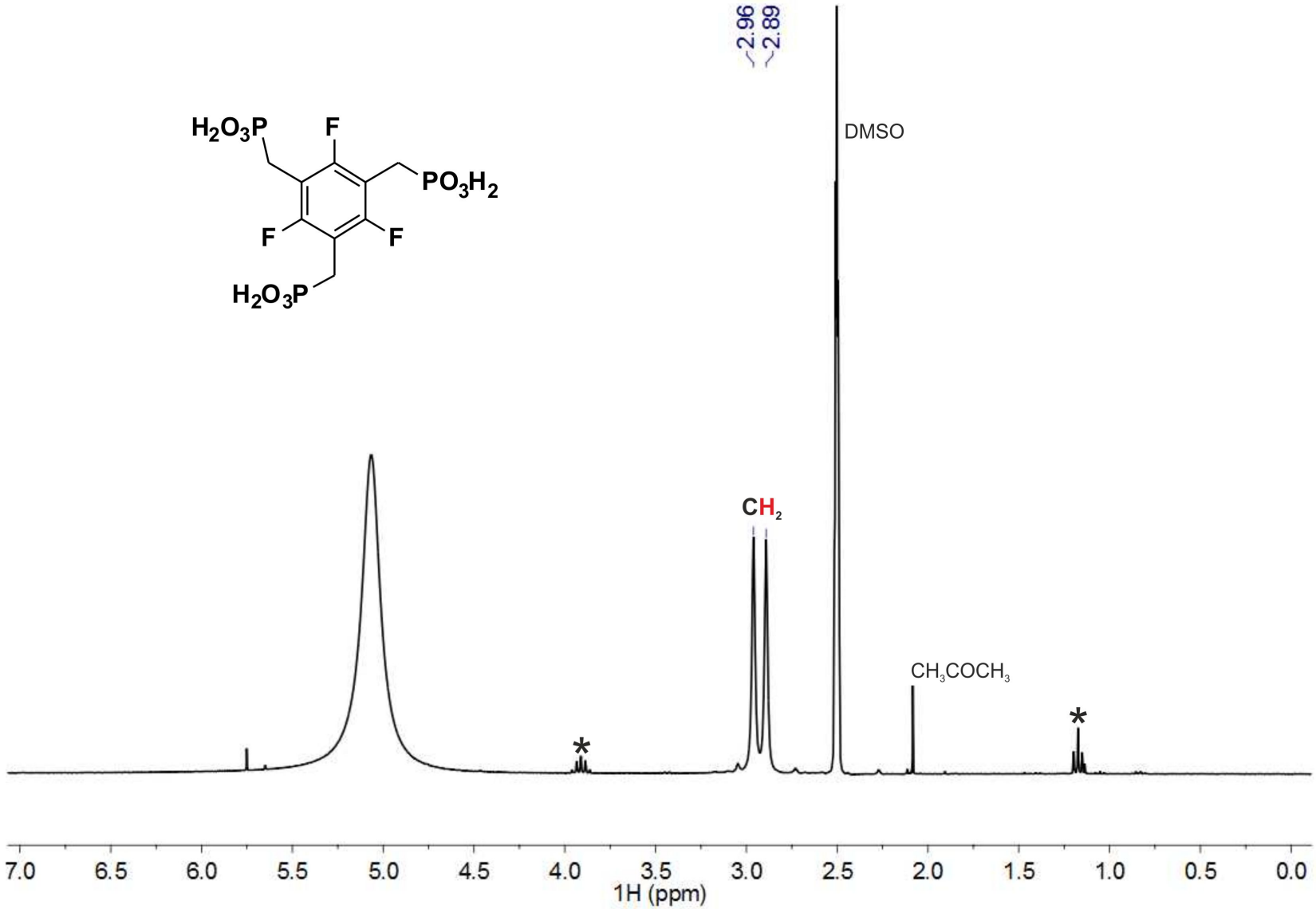

Fig. S8 ^{1}H NMR spectrum of the target molecule ((2,4,6-trifluorobenzene-1,3,5-triyl)tris(methylene))triphosphonic acid in DMSO-d_6. The asterisk identifies the presence of a small impurity, possibly corresponding to compound ***L***^{2}.

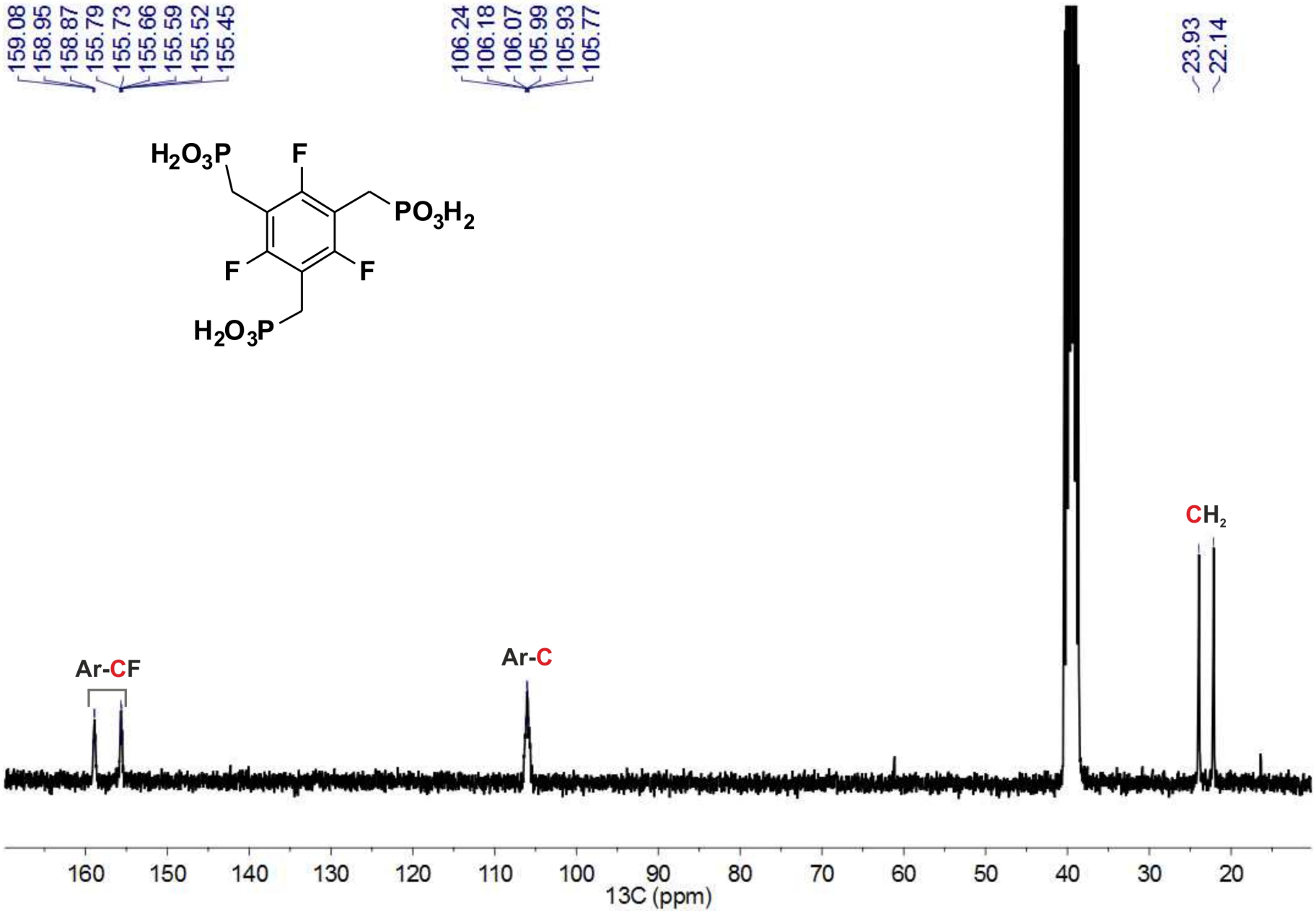

Fig. S9 ^{13}C NMR spectrum of the target molecule ((2,4,6-trifluorobenzene-1,3,5-triyl)tris(methylene))triphosphonic acid in DMSO-d_6.

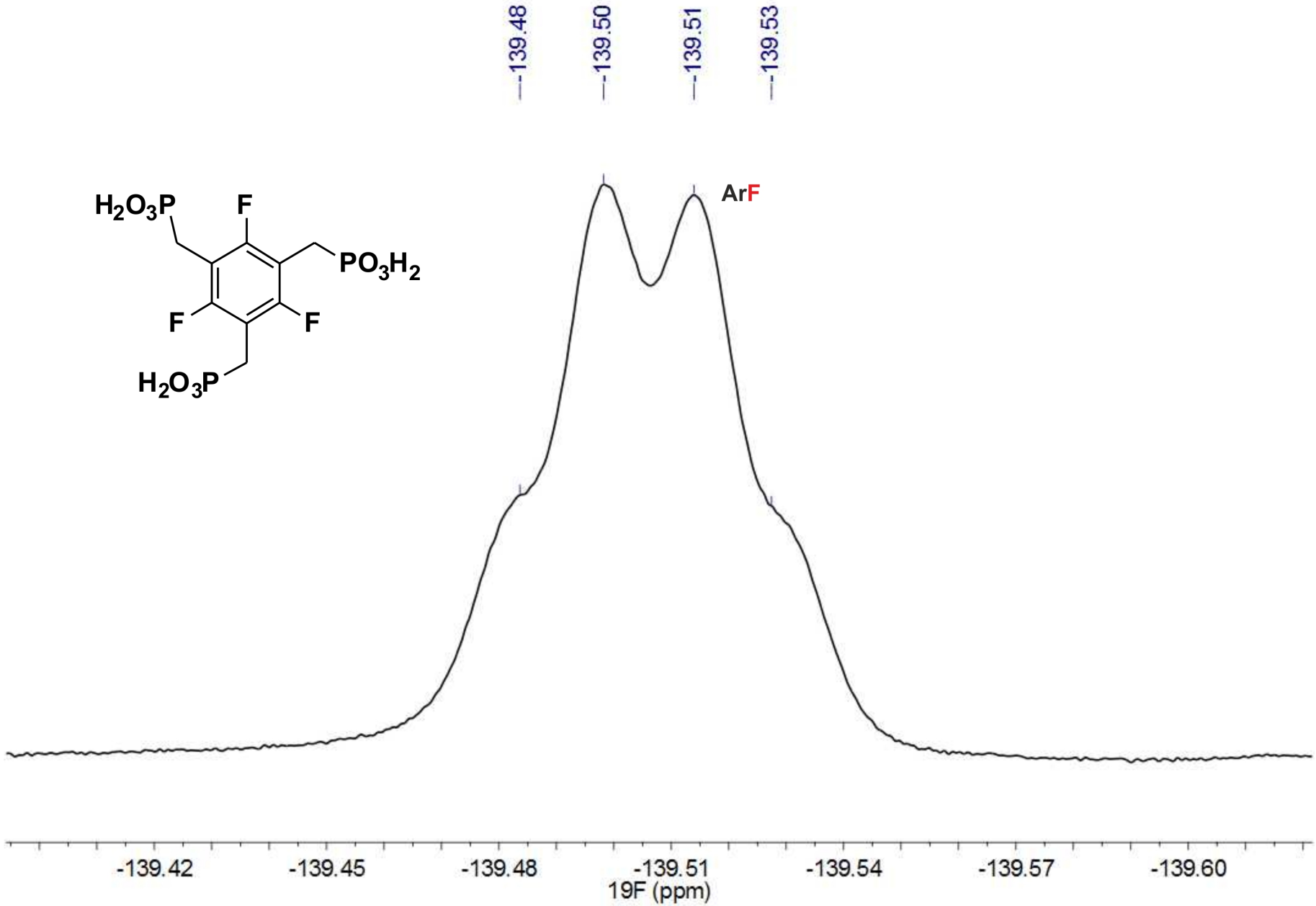

Fig. S10 ^{19}F NMR spectrum of the target molecule ((2,4,6-trifluorobenzene-1,3,5-triyl)tris(methylene))triphosphonic acid in DMSO-d_6.

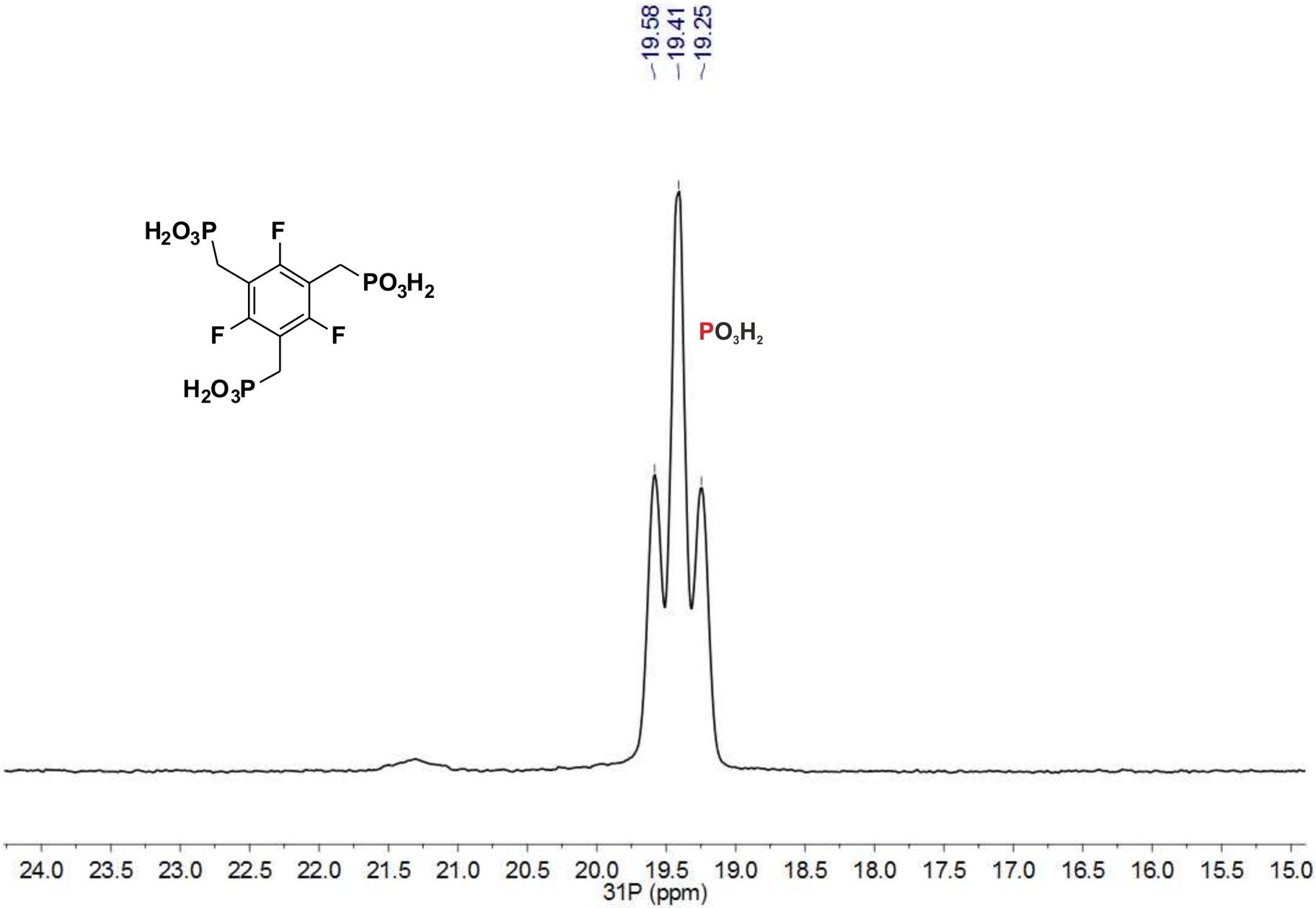

Fig. S11 ^{31}P NMR spectrum of the target molecule ((2,4,6-trifluorobenzene-1,3,5-triyl)tris(methylene))triphosphonic acid in DMSO-d_6.

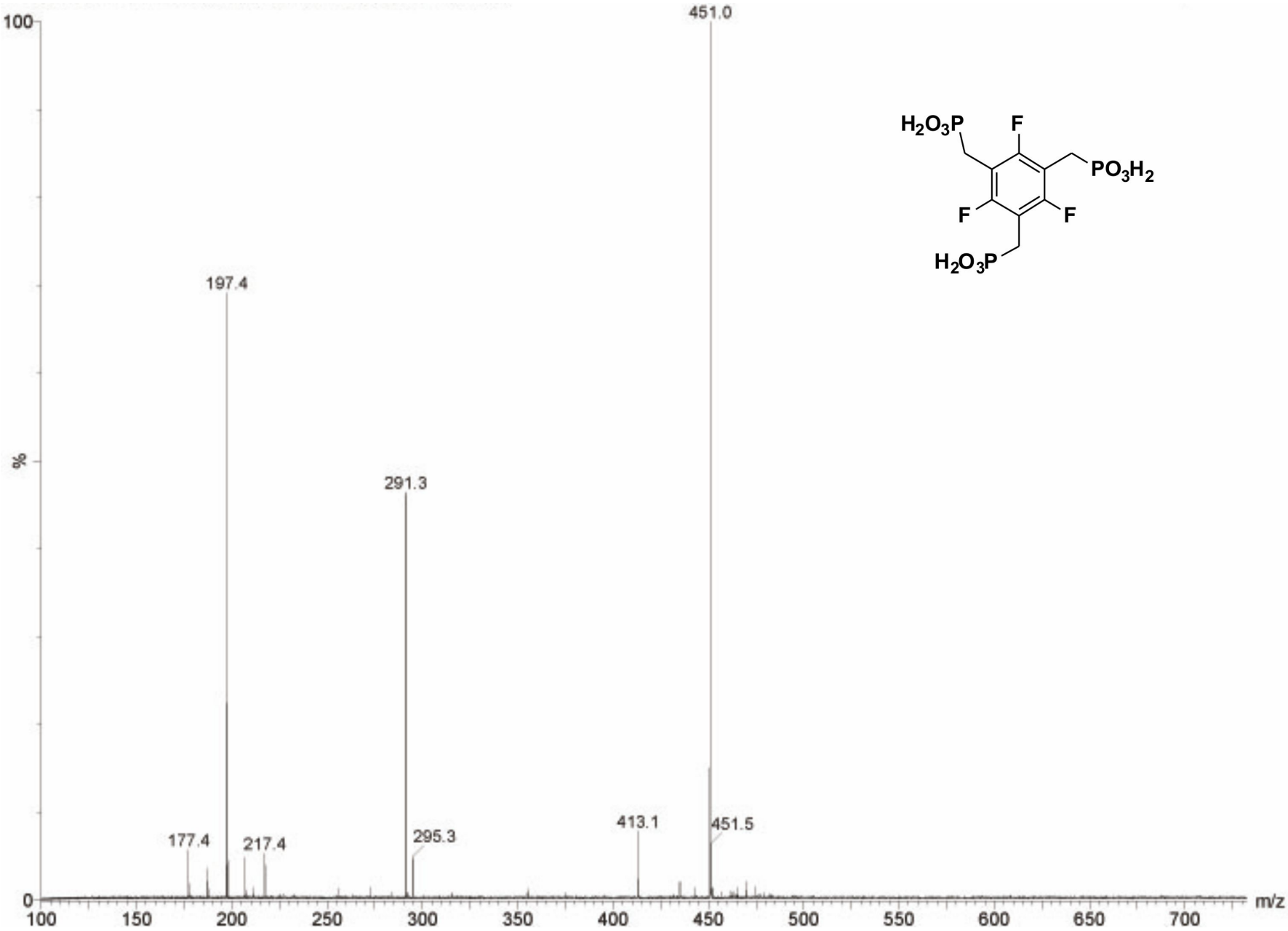

Fig. S12 Mass spectrum of the target molecule ((2,4,6-trifluorobenzene-1,3,5-triyl)tris(methylene))triphosphonic acid.

1.2. Crystal structures

1.2.1. Crystallographic details

Single crystals of 1,3,5-tris(chloromethyl)-2,4,6-trifluorobenzene (L^1), hexaethyl((2,4,6-trifluorobenzene-1,3,5-triyl)tris(methylene))tris-(phosphonate) (L^2) and ((2,4,6-trifluorobenzene-1,3,5-triyl)tris(methylene))triphosphonic acid (H_6tftp) were manually harvested from the crystallization vials. Single-crystal X-ray diffraction data were collected, processed and corrected for absorption using identical procedures as those described in section 2.5 of the main text.

Structures were solved using the direct methods algorithm implemented in SHELXS-97,[1] which allowed the immediate location of most of the non-hydrogen atoms. The remaining non-hydrogen atoms were located from difference Fourier maps calculated from successive full-matrix least-squares refinement cycles on F^2 using SHELXL-97.[1a, 2] All non-hydrogen atoms were refined anisotropically.

Hydrogen atoms belonging to the organic molecules were placed at their idealized positions around the parent atoms using appropriate HFIX *23* (–CH_2–), HFIX *137* (–CH_3 in L^2) and HFIX *147* (–OH in H_6tftp) instructions in SHELXL. Hydrogen atoms associated with the water molecules of crystallization present in the crystal structure of H_6tftp were directly located from difference Fourier maps and included in the final structural model with the O–H and H···H distances restrained to 0.95(1) and 1.55(1) Å, respectively, in order to ensure a chemically reasonable geometry for these moieties. All hydrogen atoms were included in subsequent refinement cycles in riding motion approximation with isotropic thermal displacements parameters (U_{iso}) fixed at 1.2×U_{eq} (–CH_2–) or 1.5×U_{eq} (–CH_3, –OH and H_2O) of the parent atoms.

For $\boldsymbol{L^1}$ the last difference Fourier map synthesis showed the highest peak (0.500 eÅ^{-3}) and deepest hole (-0.446 eÅ^{-3}) located at 0.69 Å and 0.44 Å from Cl3, respectively. For $\boldsymbol{L^2}$ the correspondent values were 0.529 and -0.608 eÅ^{-3}, located at 0.32 Å from C18 and 0.35 Å from H18A, respectively, and for H_6tftp the correspondent values were 0.518 and -0.381 eÅ^{-3}, located at 0.70 Å from C1 and 0.48 Å from P2. Details of the crystal data and structure refinement parameters for $\boldsymbol{L^1}$, $\boldsymbol{L^2}$ and H_6tftp are summarized in Table S1.

Crystallographic data (excluding structure factors) for the crystal structures of the new tripodal organic ligand H_6tftp, and of the two intermediate molecules, reported in this paper have been deposited with the Cambridge Crystallographic Data Centre. See CCDC deposition numbers in Table S1. Copies of the data can be obtained free of charge on application to CCDC, 12 Union Road, Cambridge CB2 2EZ, U.K. FAX: (+44) 1223 336033. E-mail: deposit@ccdc.cam.ac.uk.

Table S1 Crystal data collection and structure refinement details for the organic molecules ***L*^{1}**, ***L*^{2}** and **H_6tftp**.

	***L*^{1}**	***L*^{2}**	**H_6tftp**
Formula	$C_9H_6Cl_3F_3$	$C_{21}H_{36}F_3O_9P_3$	$C_9H_{16}F_3O_{11}P_3$
Formula weight	277.49	582.41	450.13
Temperature / K	150(2)	150(2)	150(2)
Crystal system	Orthorhombic	Triclinic	Monoclinic
Space group	$P2_12_12_1$	$P\bar{1}$	$P2_1/c$
a / Å	8.1025(3)	10.3141(6)	9.7829(5)
b / Å	8.7996(3)	10.5339(6)	9.9524(5)
c / Å	14.9510(6)	15.0122(10)	17.0510(9)
α / º	90	69.566(3)	90.00
β / º	90	71.856(3)	100.424(2)
γ / º	90	69.669(3)	90.00
Volume / Å^3	1065.99(7)	1399.25(15)	1632.74(15)
Z	4	2	4
D_c/g cm^{-3}	1.729	1.382	1.831
μ(Mo-Kα) / mm^{-1}	0.861	0.277	0.455
Crystal size / mm^3	0.13×0.11×0.08	0.09×0.04×0.02	0.12×0.09×0.05
Crystal type	Colourless block	Colourless plate	Colourless block
θ range (º)	3.58 to 33.08	3.69 to 29.13	3.57 to 33.14
Index ranges	$-12 \le h \le 11$ $-10 \le k \le 13$ $-22 \le l \le 22$	$-14 \le h \le 12$ $-14 \le k \le 14$ $-20 \le l \le 20$	$-15 \le h \le 14$ $-15 \le k \le 15$ $-26 \le l \le 26$
Reflections collected	18734	24478	68711
Independent reflections	4042 [R_{int} = 0.0279]	7427 [R_{int} =0.0505]	6206 [R_{int} = 0.0309]
Completeness	99.8 % (to θ=33.08º)	98.6 % (to θ=29.13º)	99.6 % (to θ=33.14º)
Final R indices [I>2σ(I)] [a,b]	$R1$ = 0.0314 $wR2$ = 0.0671	$R1$ = 0.0520 $wR2$ = 0.1122	$R1$ = 0.0345 $wR2$ = 0.0924
Final R indices (all data) [a,b]	$R1$ = 0.0399, $wR2$ = 0.0717	$R1$ = 0.1017, $wR2$ = 0.1298	$R1$ = 0.0449, $wR2$ = 0.0997
Weighting scheme[c]	m=0.0275 n=0.3250	m=0.0559 n=0.3264	m=0.0496 n=0.7191
Largest diff. peak and hole	0.500 and -0.446 eÅ^{-3}	0.529 and -0.608 eÅ^{-3}	0.518 and -0.381 eÅ^{-3}
CCDC no.	952454	952455	952453

$^{a}\, R1 = \sum \left\| F_o \right| - \left| F_c \right\| / \sum \left| F_o \right|$; $^{b}\, wR2 = \sqrt{\sum \left[w\left(F_o^2 - F_c^2\right)^2 \right] / \sum \left[w\left(F_o^2\right)^2 \right]}$

$^{c}\, w = 1 / \left[\sigma^2\left(F_o^2\right) + \left(mP\right)^2 + nP \right]$ where $P = \left(F_o^2 + 2F_c^2\right)/3$

1.2.2. 1,3,5-Tris(chloromethyl)-2,4,6-trifluorobenzene (*L*[1])

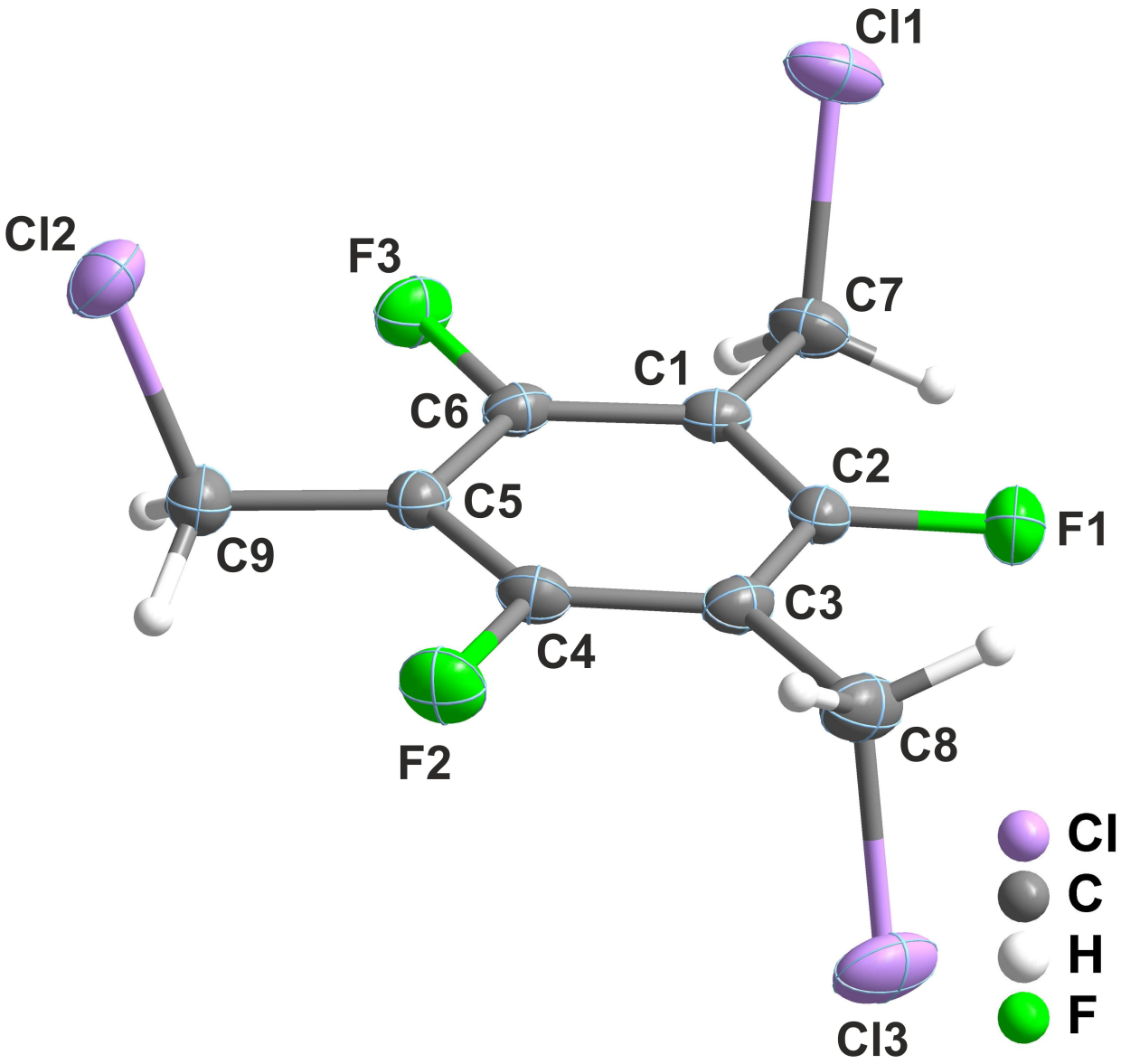

Fig. S13 Molecular structure of 1,3,5-tris(chloromethyl)-2,4,6-trifluorobenzene (***L***[1]) showing the atomic labeling scheme for all non-hydrogen atoms. Displacement ellipsoids are drawn at the 50% probability level.

1.2.3. Hexaethyl((2,4,6-trifluorobenzene-1,3,5-triyl)tris(methylene))tris-(phosphonate) (*L*^{2})

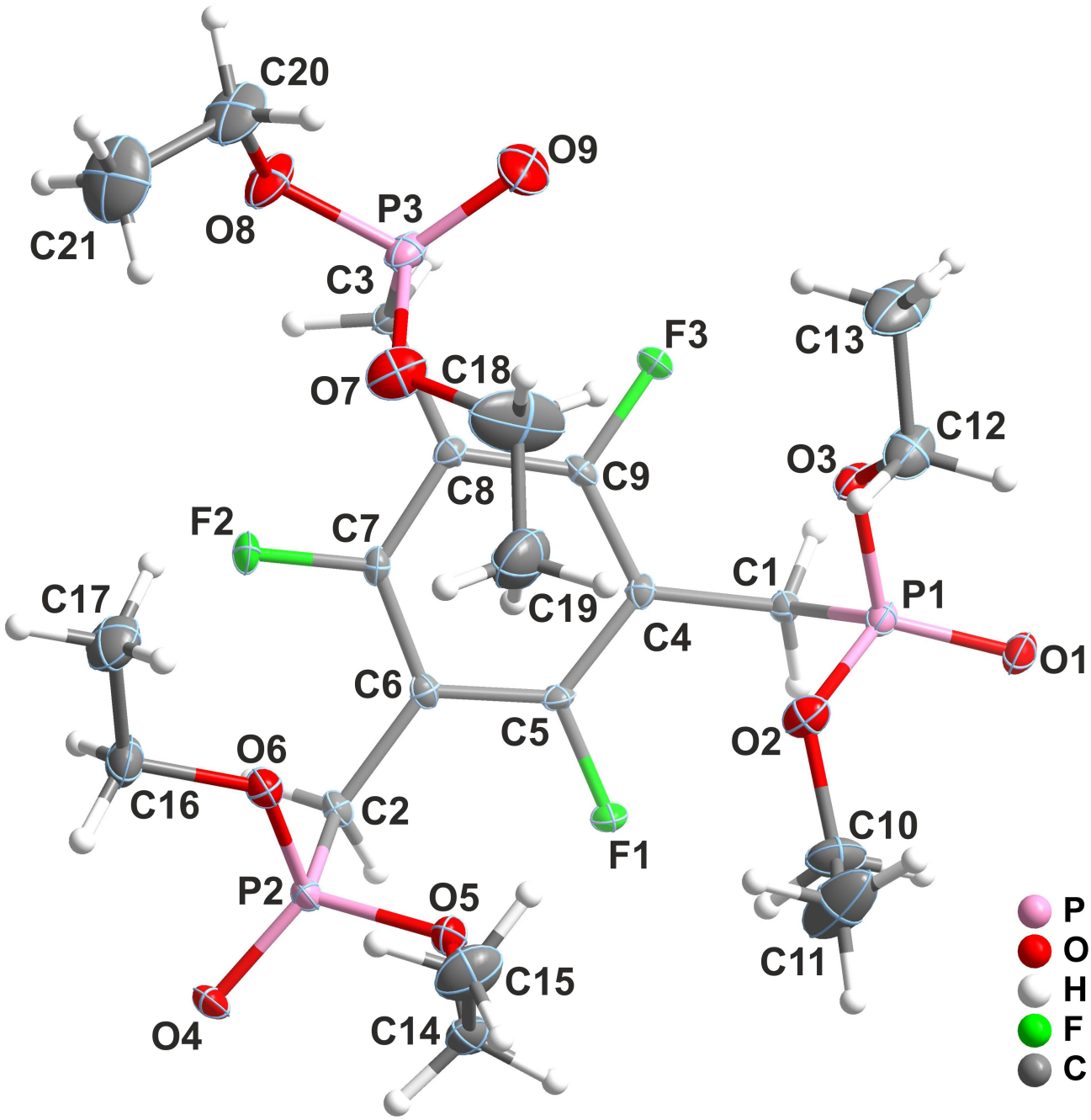

Fig. S14 Molecular structure of hexaethyl((2,4,6-trifluorobenzene-1,3,5-triyl)tris-(methylene))tris(phosphonate) (*L*^{2}) showing the atomic labeling scheme for all non-hydrogen atoms. Displacement ellipsoids are drawn at the 30% probability level.

1.2.4. ((2,4,6-Trifluorobenzene-1,3,5-triyl)tris(methylene))triphosphonic acid (H_6tftp)

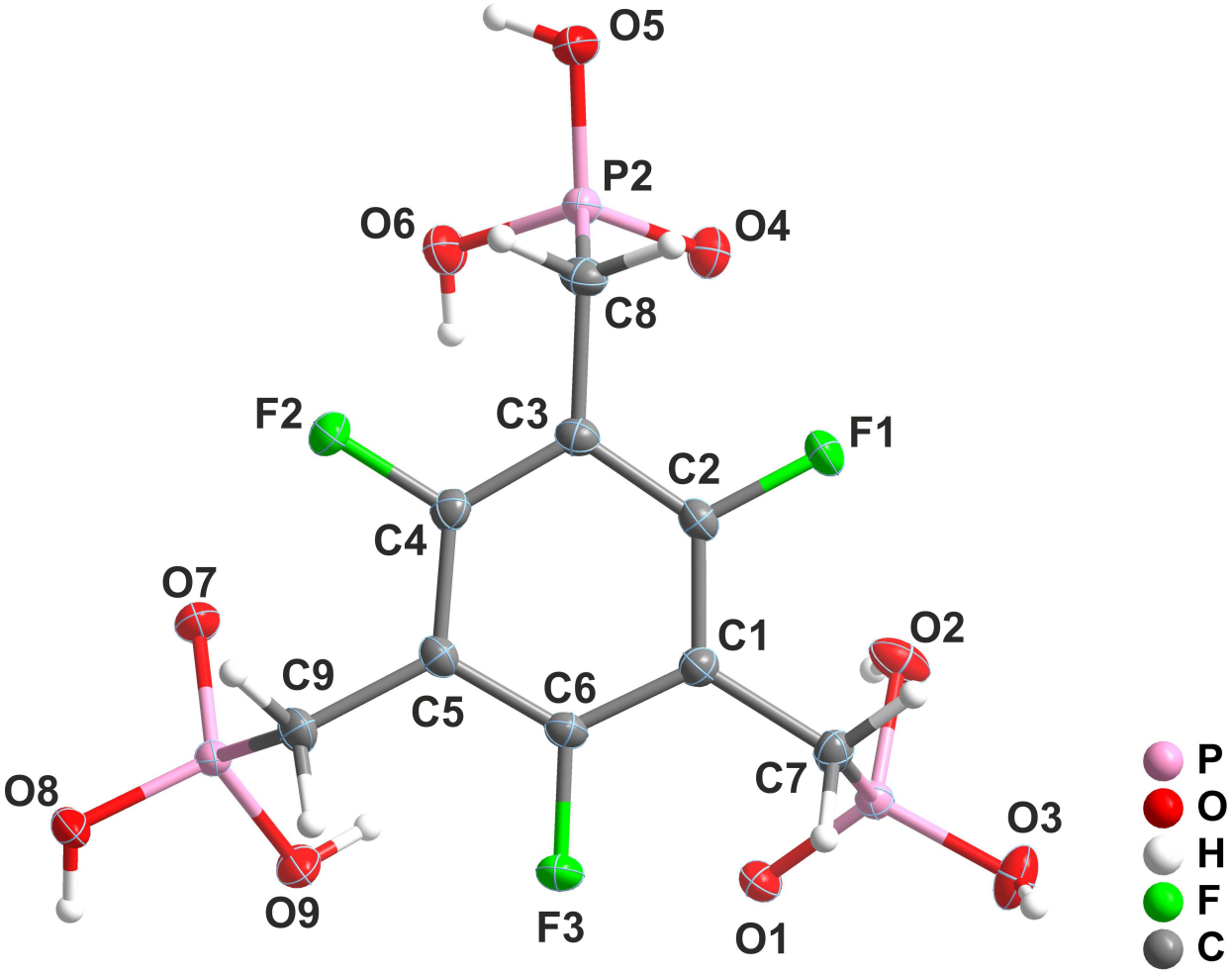

Fig. S15 Molecular structure of ((2,4,6-trifluorobenzene-1,3,5-triyl)tris(methylene))-triphosphonic acid (**H_6tftp**) showing the atomic labeling scheme for all non-hydrogen atoms. Displacement ellipsoids are drawn at the 50% probability level.

2. Electron Microscopy Studies: EDS Mapping

2.1. $[(La_{0.95}Eu_{0.05})(H_3tftp)(H_2O)]$ (2)

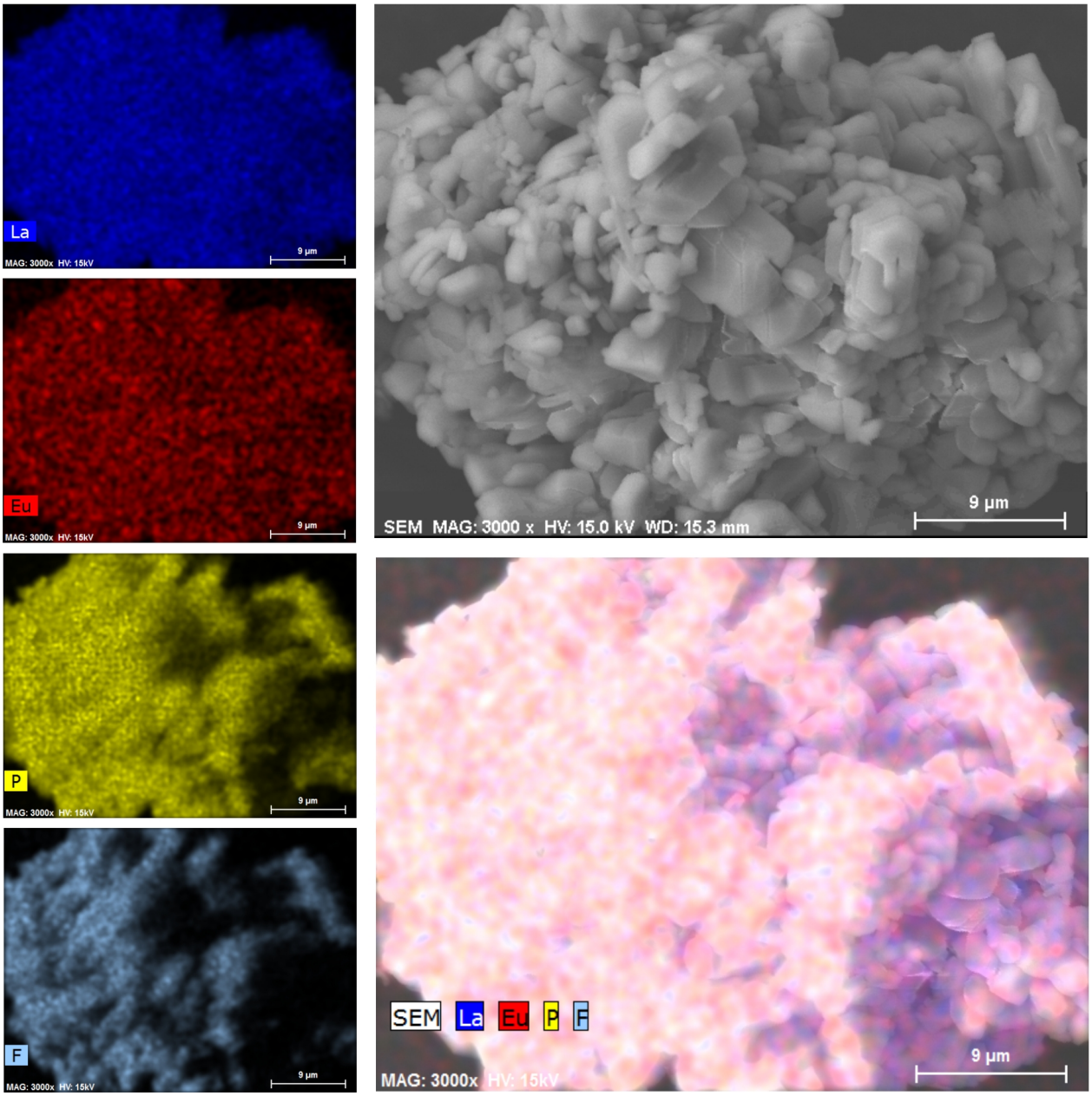

Fig. S16 Electron microscopy EDS mapping studies of a portion of the mixed-lanthanide photoluminescent $[(La_{0.95}Eu_{0.05})(H_3tftp)(H_2O)]$ (**2**) material.

2.2. $[(La_{0.95}Tb_{0.05})(H_3tftp)(H_2O)]$ (3)

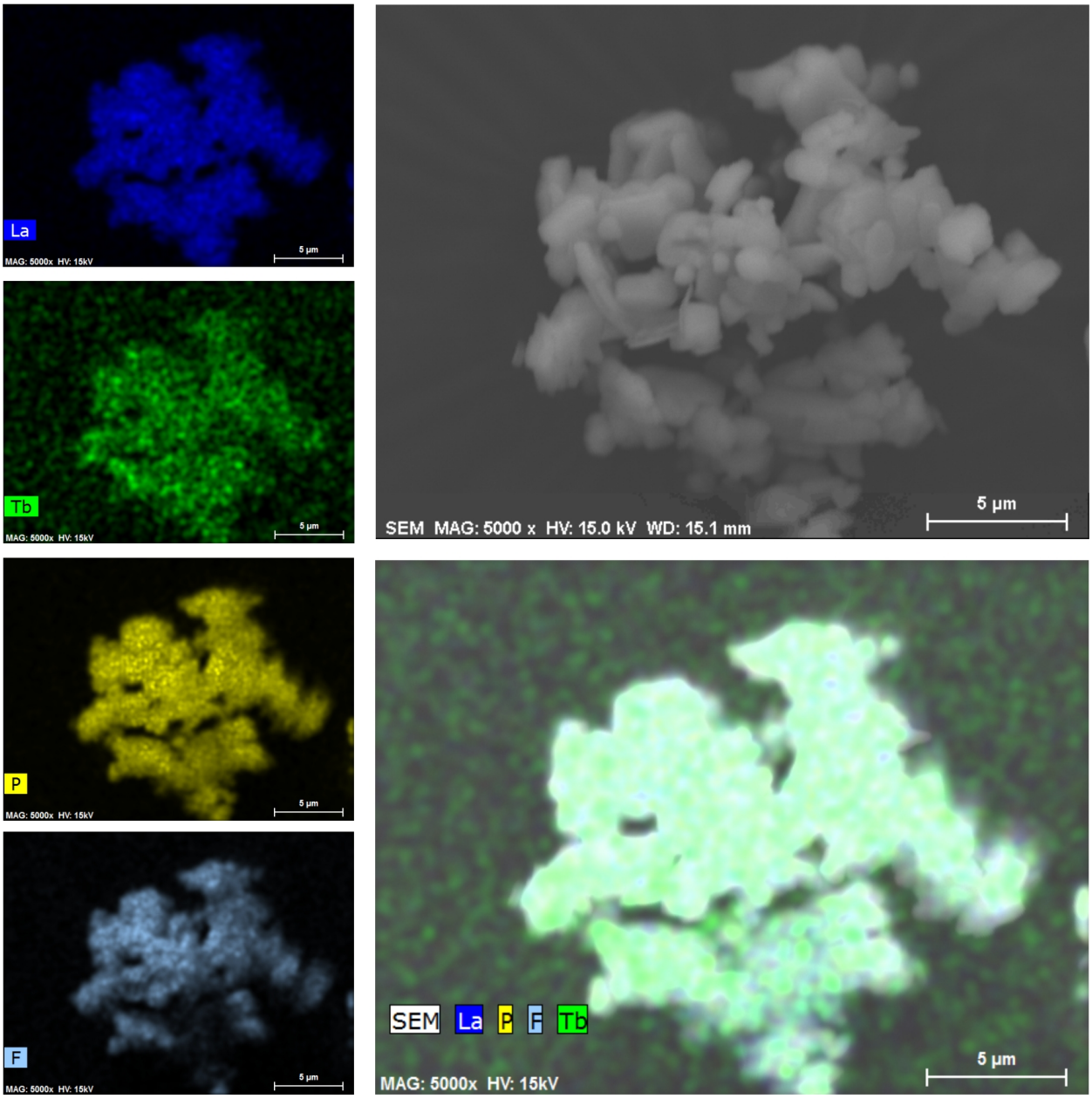

Fig. S17 Electron microscopy EDS mapping studies of a portion of the mixed-lanthanide photoluminescent $[(La_{0.95}Tb_{0.05})(H_3tftp)(H_2O)]$ (**3**) material.

2.3. $[(La_{0.94}Eu_{0.03}Tb_{0.03})(H_3tftp)(H_2O)]$ (4)

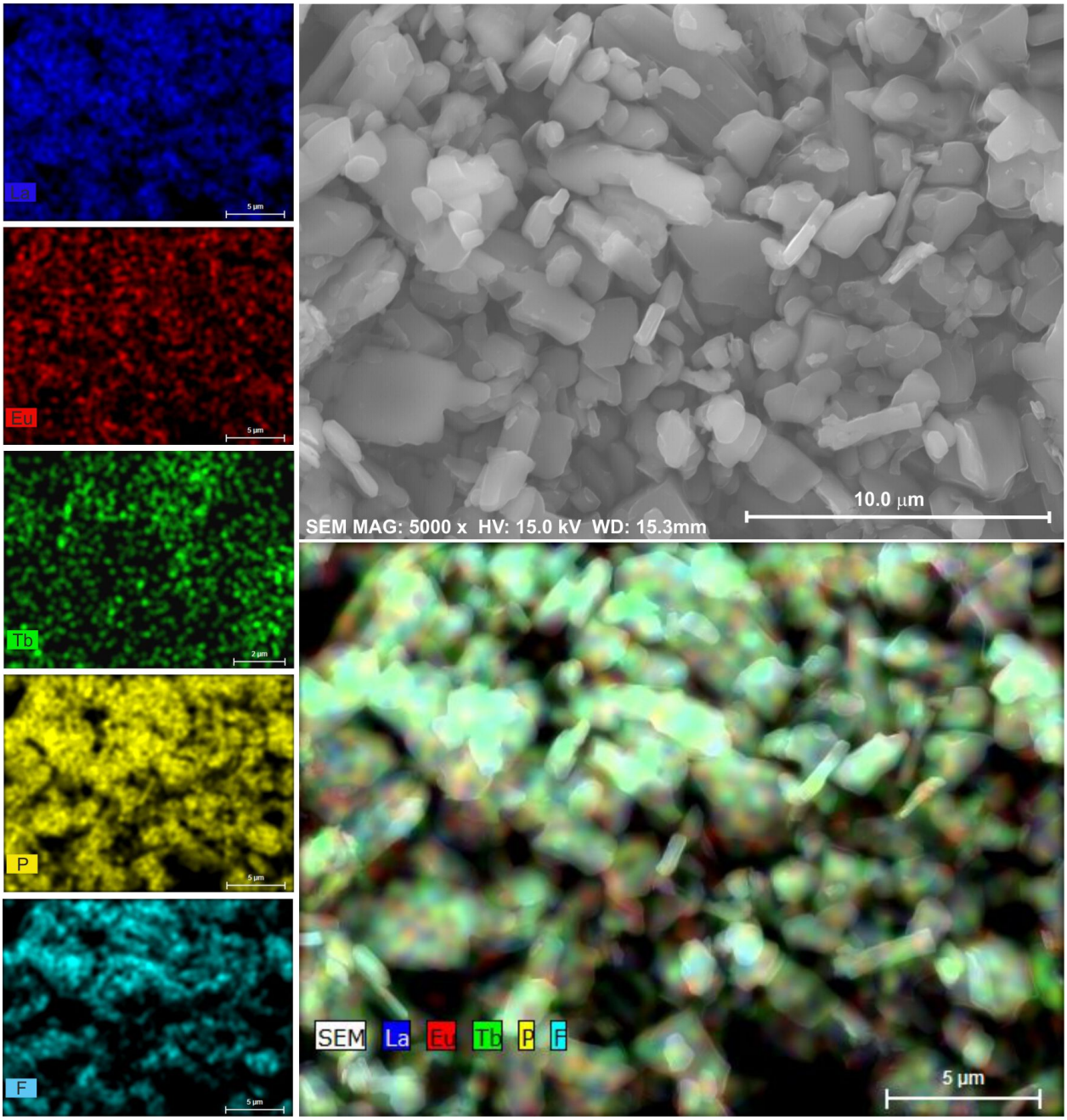

Fig. S18 Electron microscopy EDS mapping studies of a portion of the mixed-lanthanide photoluminescent $[(La_{0.94}Eu_{0.03}Tb_{0.03})(H_3tftp)(H_2O)]$ (**4**) material.

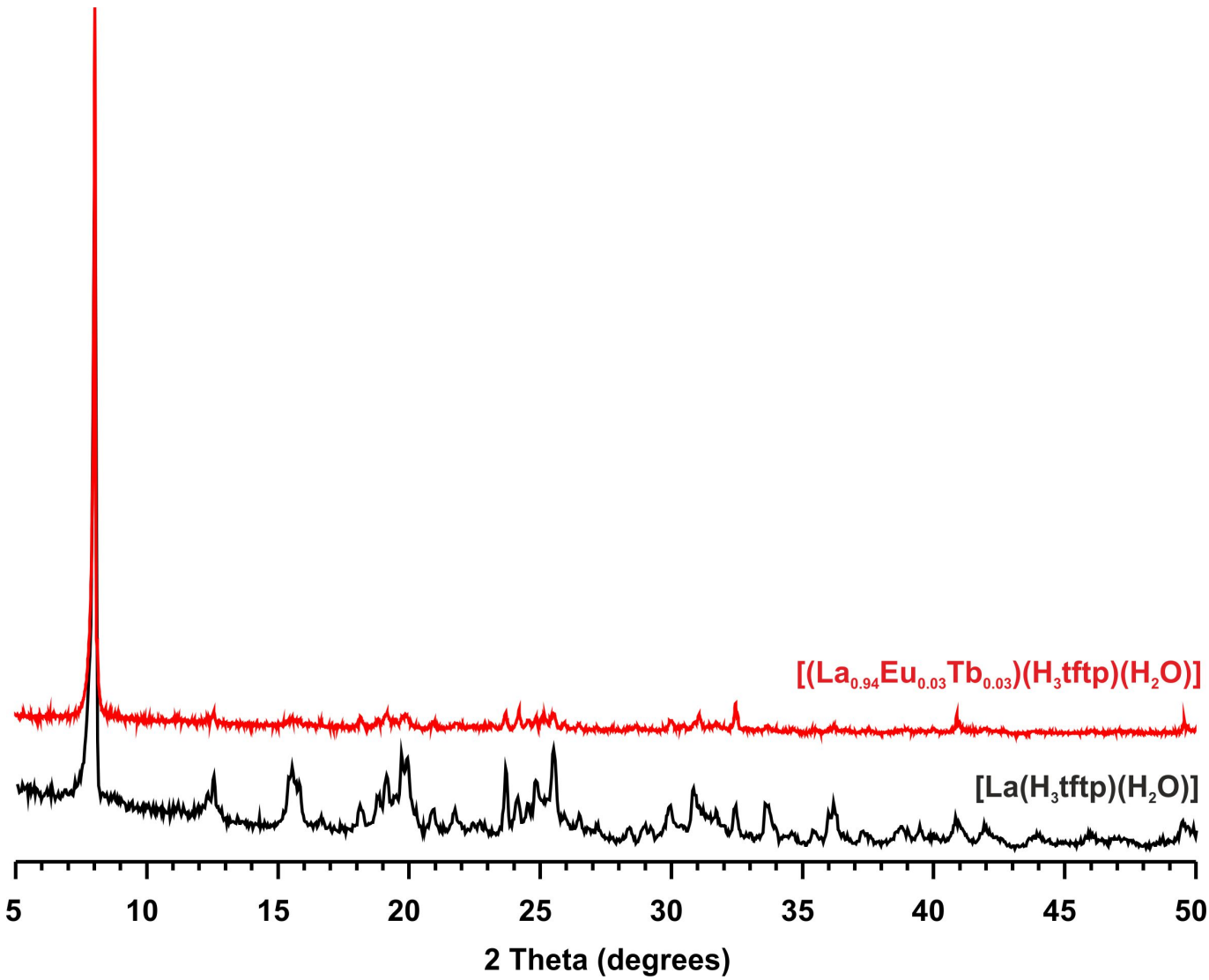

Fig. S19 Powder X-ray diffraction pattern of [La(H_3tftp)(H_2O)] (**1**) and [($La_{0.94}Eu_{0.03}Tb_{0.03}$)($H_3$tftp)($H_2O$)] (**4**) materials prepared (under hydrothermal conditions) at 180 ºC for 72 h.

3. Additional crystallographic representations: [La(H_3tftp)(H_2O)]

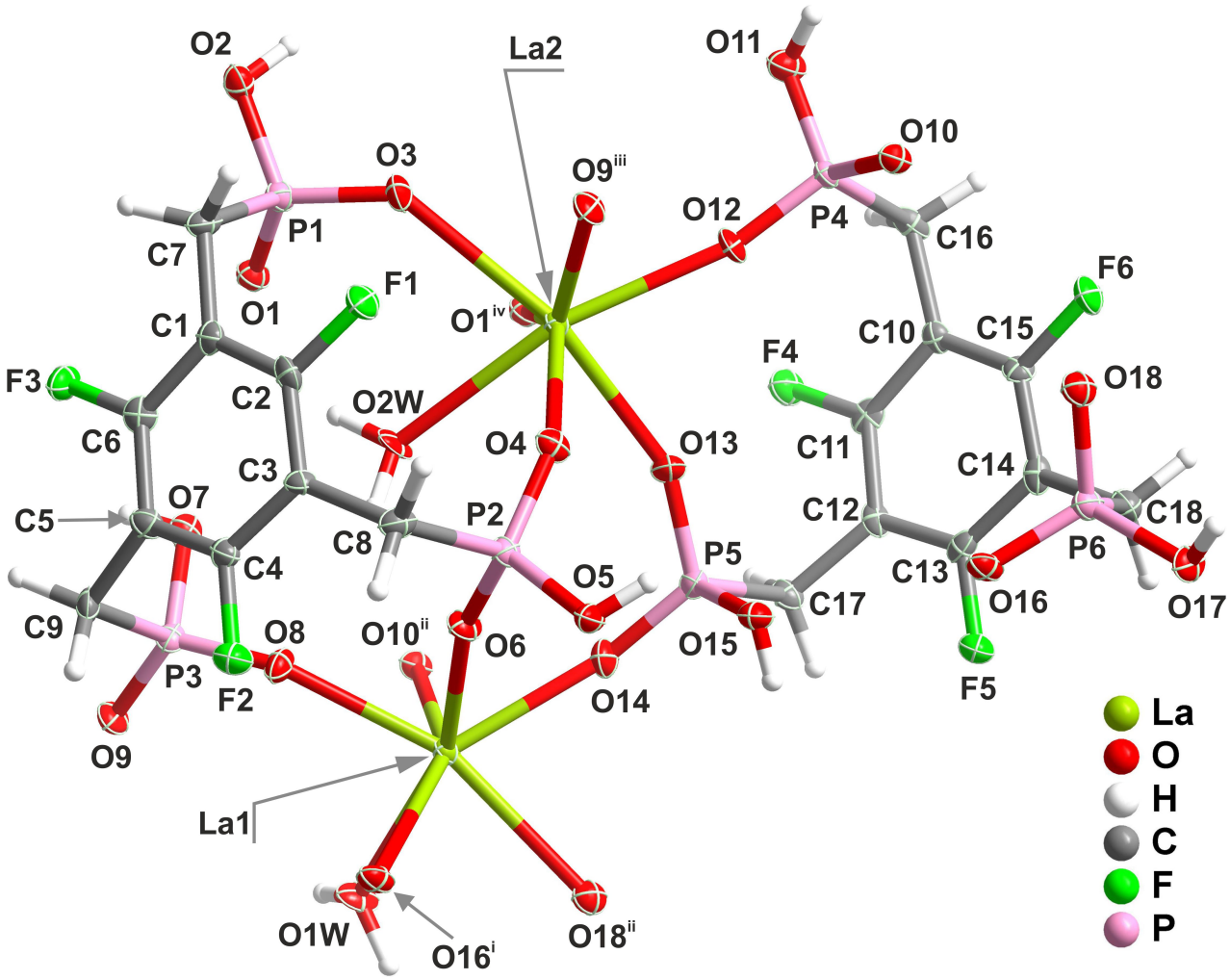

Fig. S20 Schematic representation of the asymmetric unit of [La(H_3tftp)(H_2O)] (**1**) showing all non-hydrogen atoms represented as thermal ellipsoids drawn at 50% probability level and hydrogen atoms as small spheres with arbitrary radii. The coordination environments around the two crystallographically independent metal centers have been completed for the sake of clarity. For selected bond lengths and angles on the two {LaO_7} monocapped trigonal prismatic coordination environments see Table 2 in the main manuscript. Symmetry transformations used to generate equivalent atoms: (i) –*x*, 2-*y*, 2-*z*; (ii) -1+*x*, *y*, *z*; (iii) 1+*x*, *y*, *z*; (iv) –*x*, 2-*y*, 1-*z*.

4. Solid-State NMR: [La(H_3tftp)(H_2O)]

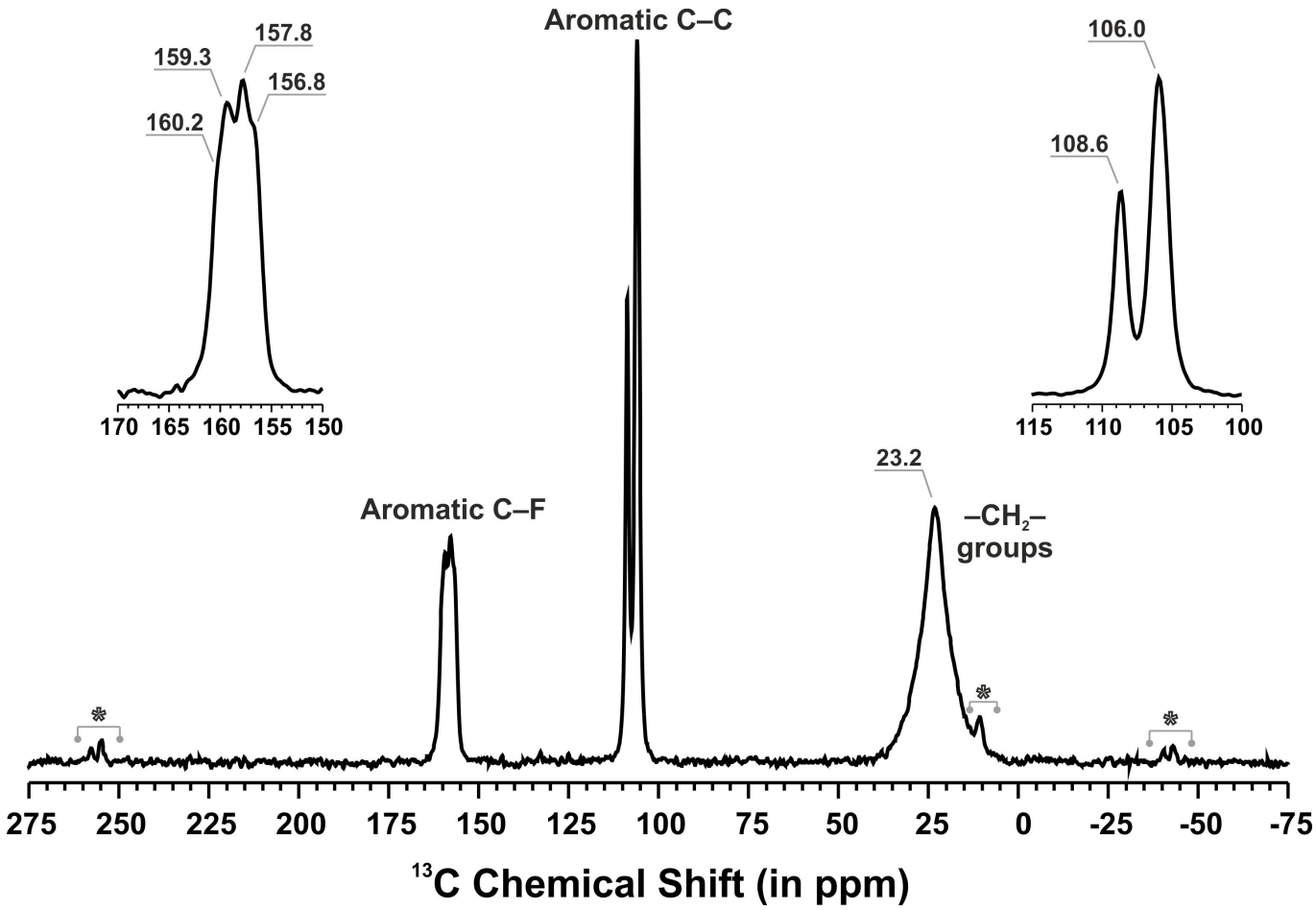

Fig. S21 $^{13}C\{^1H\}$ CP MAS spectrum of [La(H_3tftp)(H_2O)] (**1**). Spinning sidebands are denoted using an asterisk.

5. FT-IR Spectroscopy

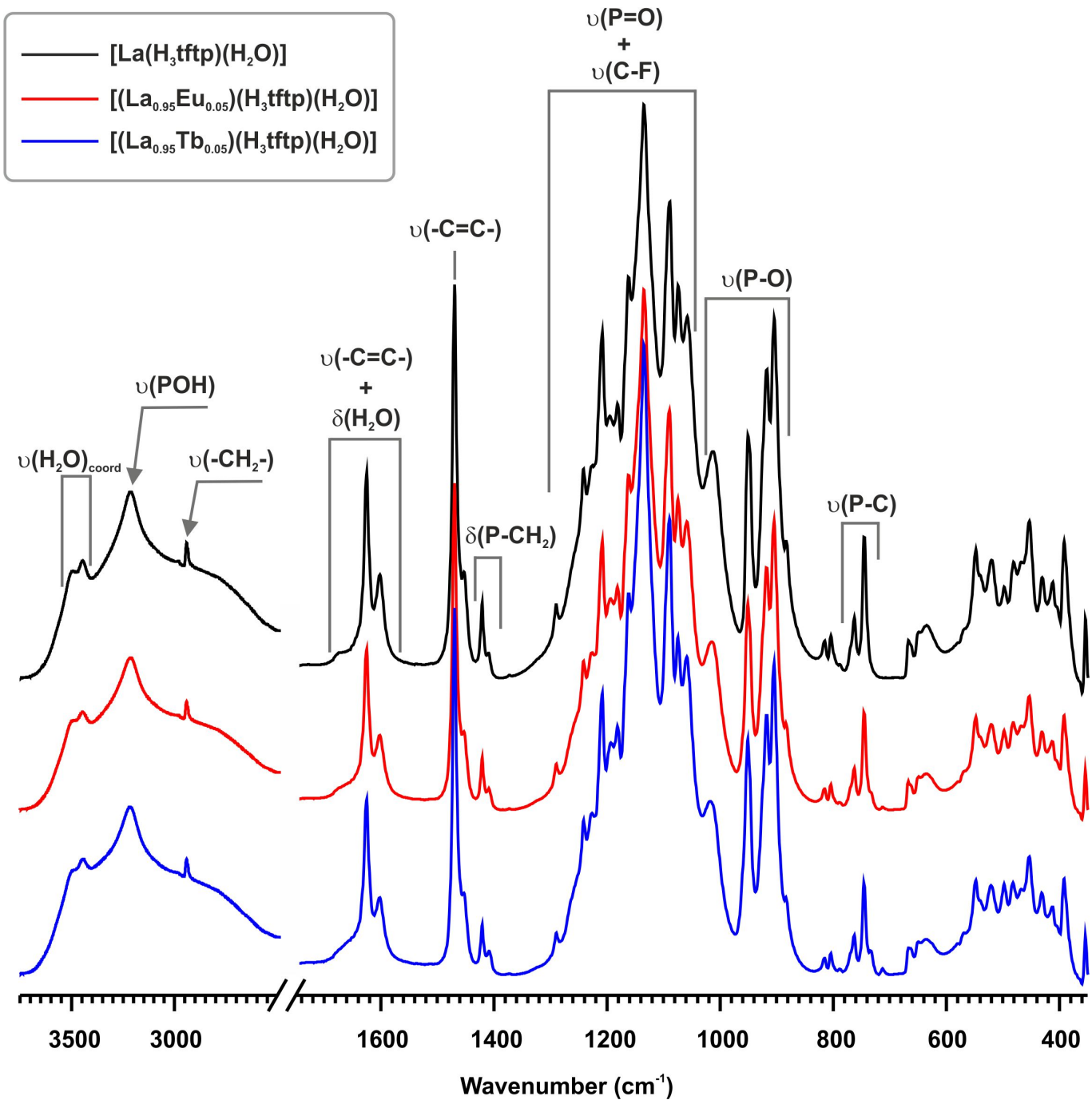

Fig. S22 FT-IR spectra of the isotypical series of [Ln(H_3tftp)(H_2O)] materials [where Ln^{3+} = La^{3+} (**1**), $(La_{0.95}Eu_{0.05})^{3+}$ (**2**) and $(La_{0.95}Tb_{0.05})^{3+}$ (**3**)].

6. Thermogravimetry

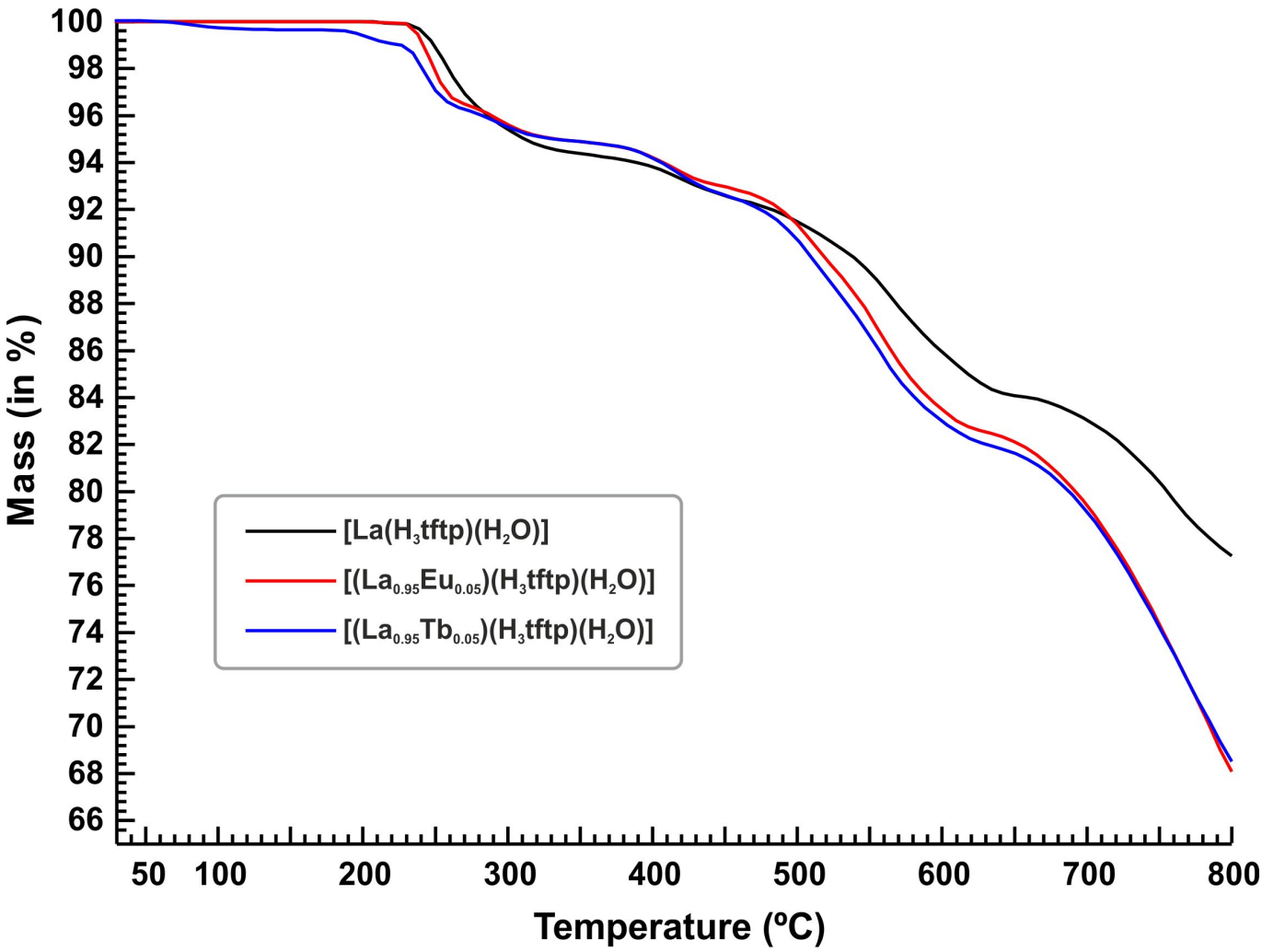

Fig. S23 Thermogravimetric curves of the isotypical series of [Ln(H_3tftp)(H_2O)] materials [where $Ln^{3+} = La^{3+}$ (**1**), $(La_{0.95}Eu_{0.05})^{3+}$ (**2**) and $(La_{0.95}Tb_{0.05})^{3+}$ (**3**)].

7. Photoluminescence

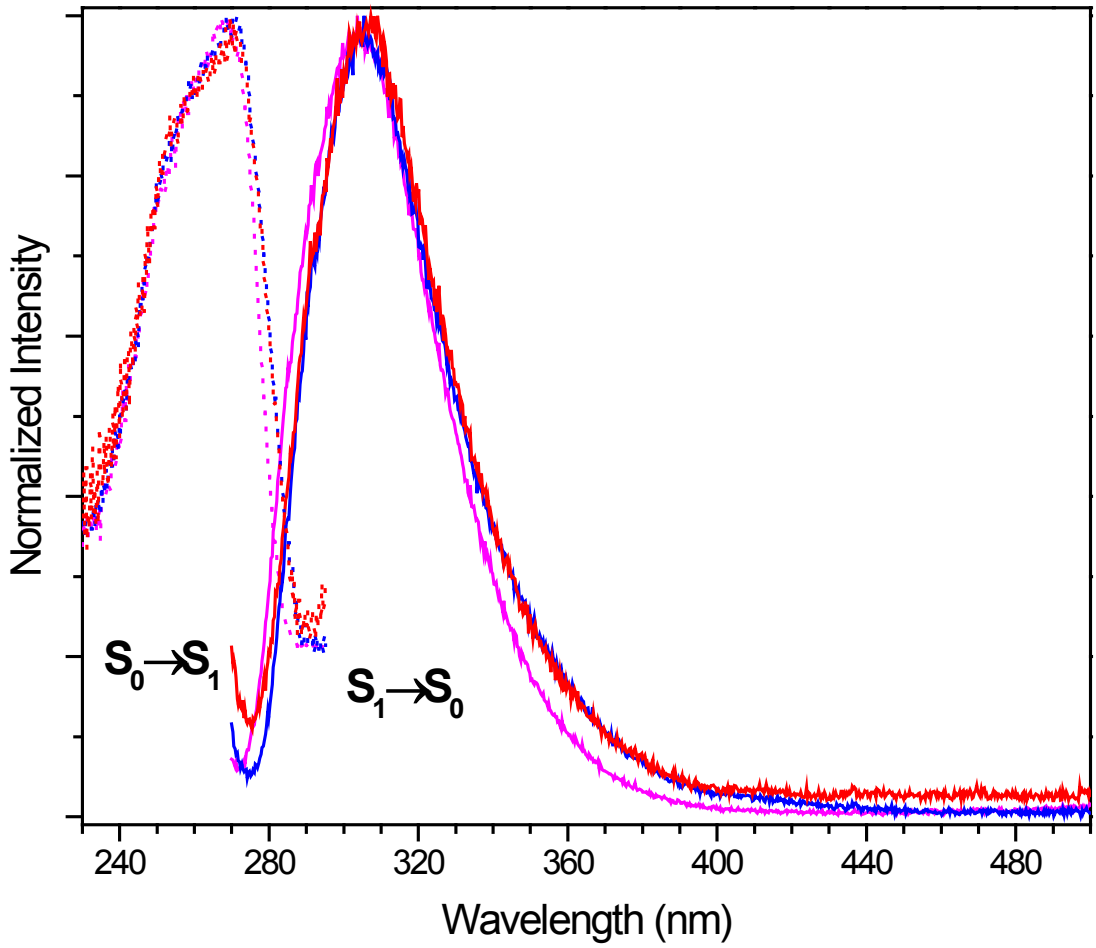

Fig. S24 Excitation and emission UV fluorescence spectra of the H_6tftp ligand (magenta), [La(H_3tftp)(H_2O)] (**1**) (blue) and [($La_{0.95}Eu_{0.05}$)(H_3tftp)(H_2O)] (**2**) (red) compounds recorded at ambient temperature. For the excitation spectra the emission was detected at 330 nm (dotted lines) while for the emission spectra (solid lines) the excitation was fixed at 265 nm.

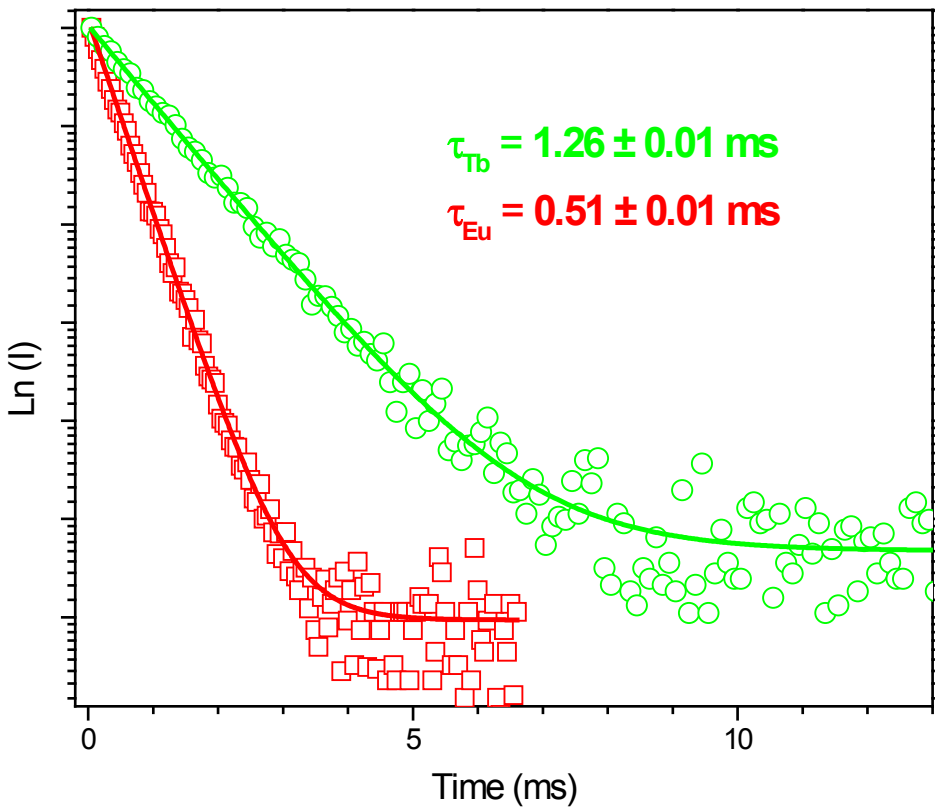

Fig. S25 $^5D_0$ and $^5D_4$ decay curves of the mixed-lanthanide [($La_{0.95}Eu_{0.05}$)(H_3tftp)(H_2O)] (**2**) (red line) and [($La_{0.95}Tb_{0.05}$)(H_3tftp)(H_2O)] (**3**) (green line) materials acquired at ambient temperature (298 K), while monitoring the emission at 610 and 542 nm, respectively. Data have been fitted with single exponential decay functions. The excitation was performed at 393 and 376 nm for **2** and **3**, respectively.

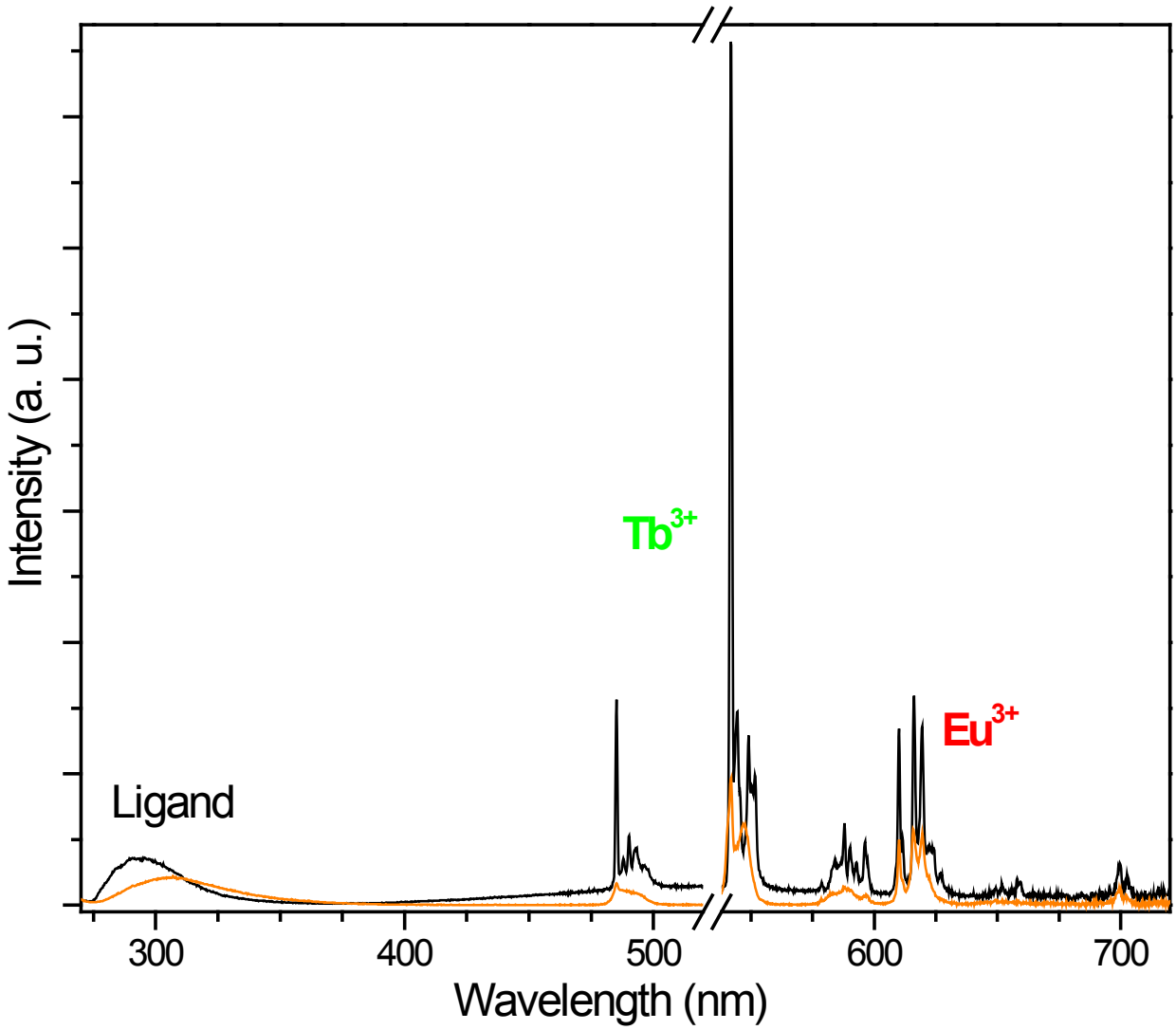

Fig. S26 UV/Vis emission spectra of $[(La_{0.94}Eu_{0.03}Tb_{0.03})(H_3tftp)(H_2O)]$ (**4**) recorded at ambient temperature (orange line) and at 12 K (black line). Excitation at 265 nm. The break in the graph indicates the second order excitation position.

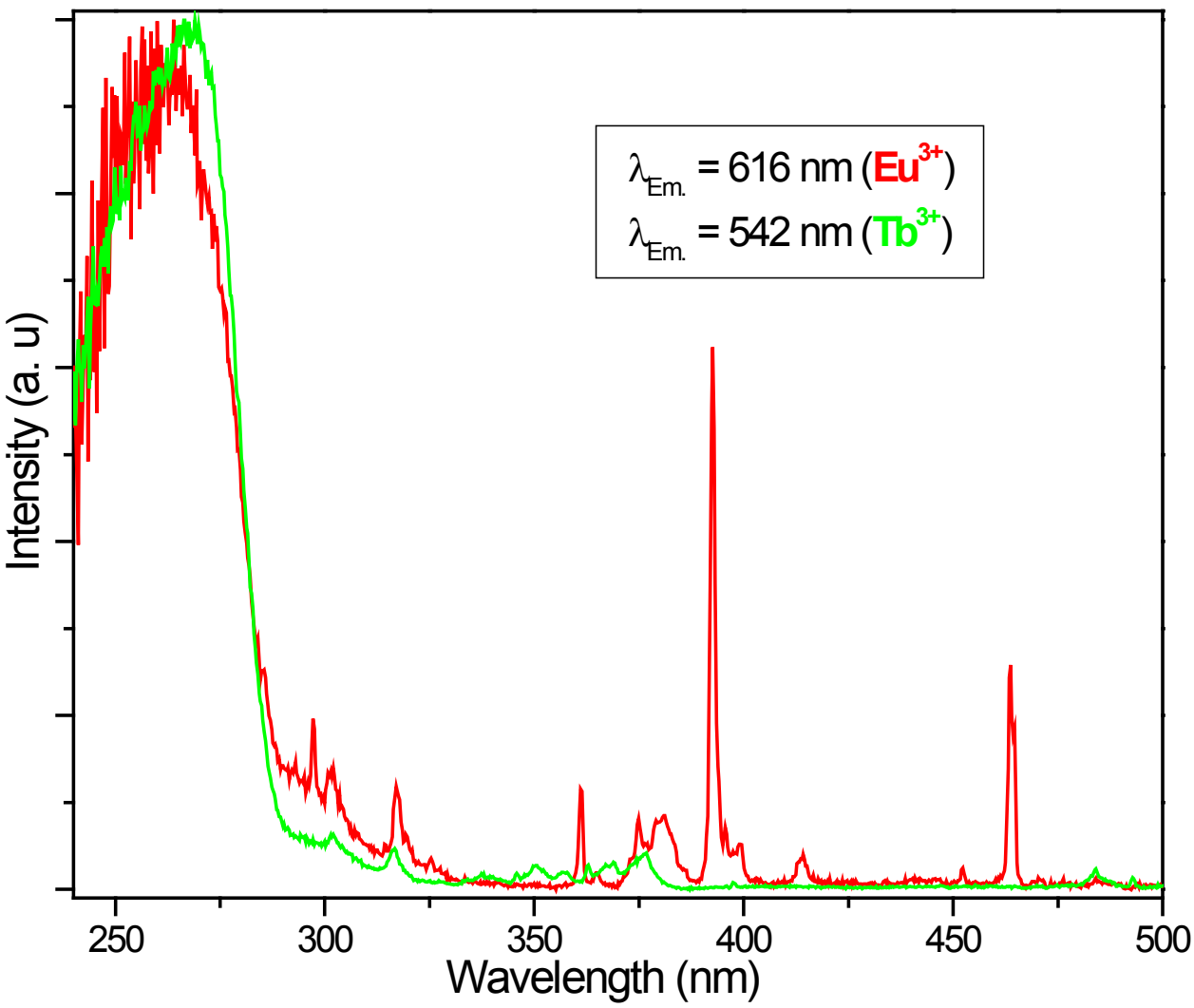

Fig. S27 Excitation spectra of $[(La_{0.94}Eu_{0.03}Tb_{0.03})(H_3tftp)(H_2O)]$ (**4**) recorded at ambient temperature (296 K) while detecting the Eu^{3+} and Tb^{3+} emission at 616 and 542 nm, respectively.

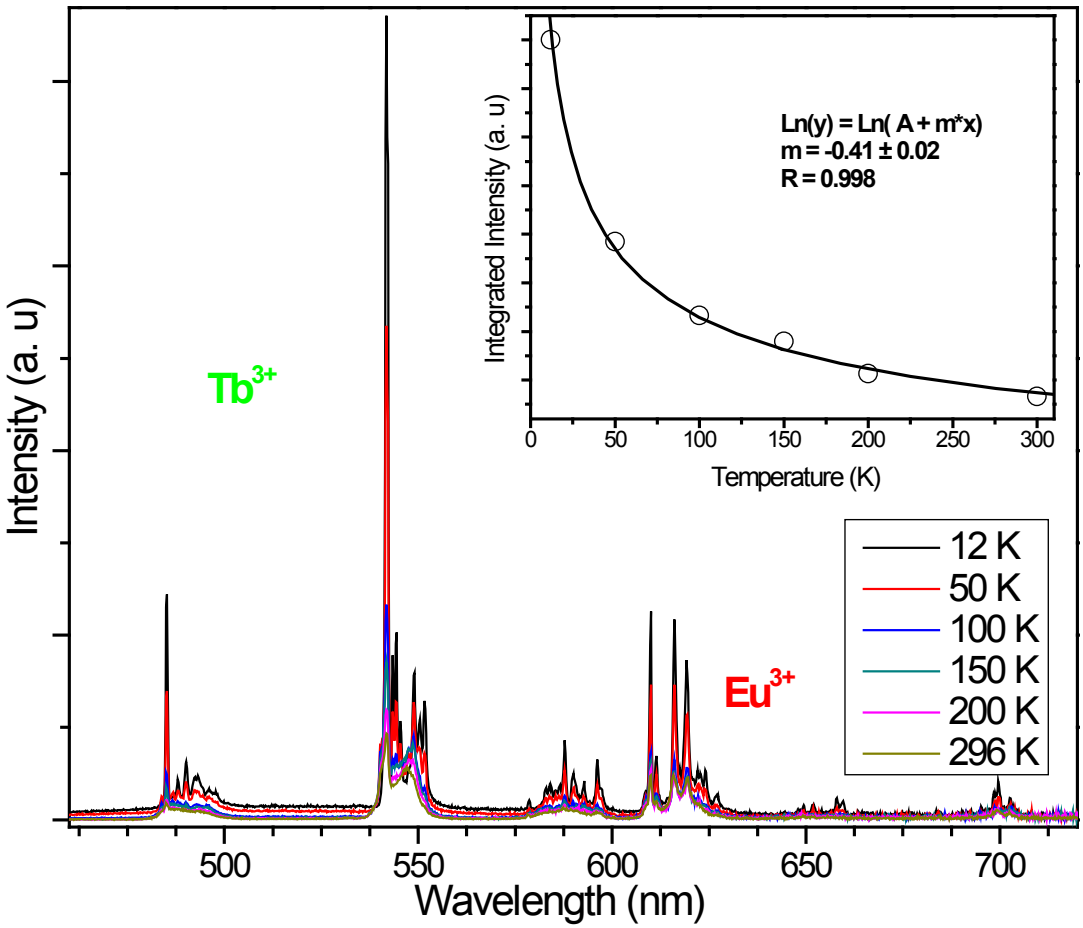

Fig. S28 Visible emission spectra of $[(La_{0.94}Eu_{0.03}Tb_{0.03})(H_3tftp)(H_2O)]$ (**4**) excited at 265 nm as a function of temperature. The inset shows the plot of the integrated intensity *vs.* temperature, and the corresponding fit after logarithmic linearization of the temperature and integrated emission intensities.

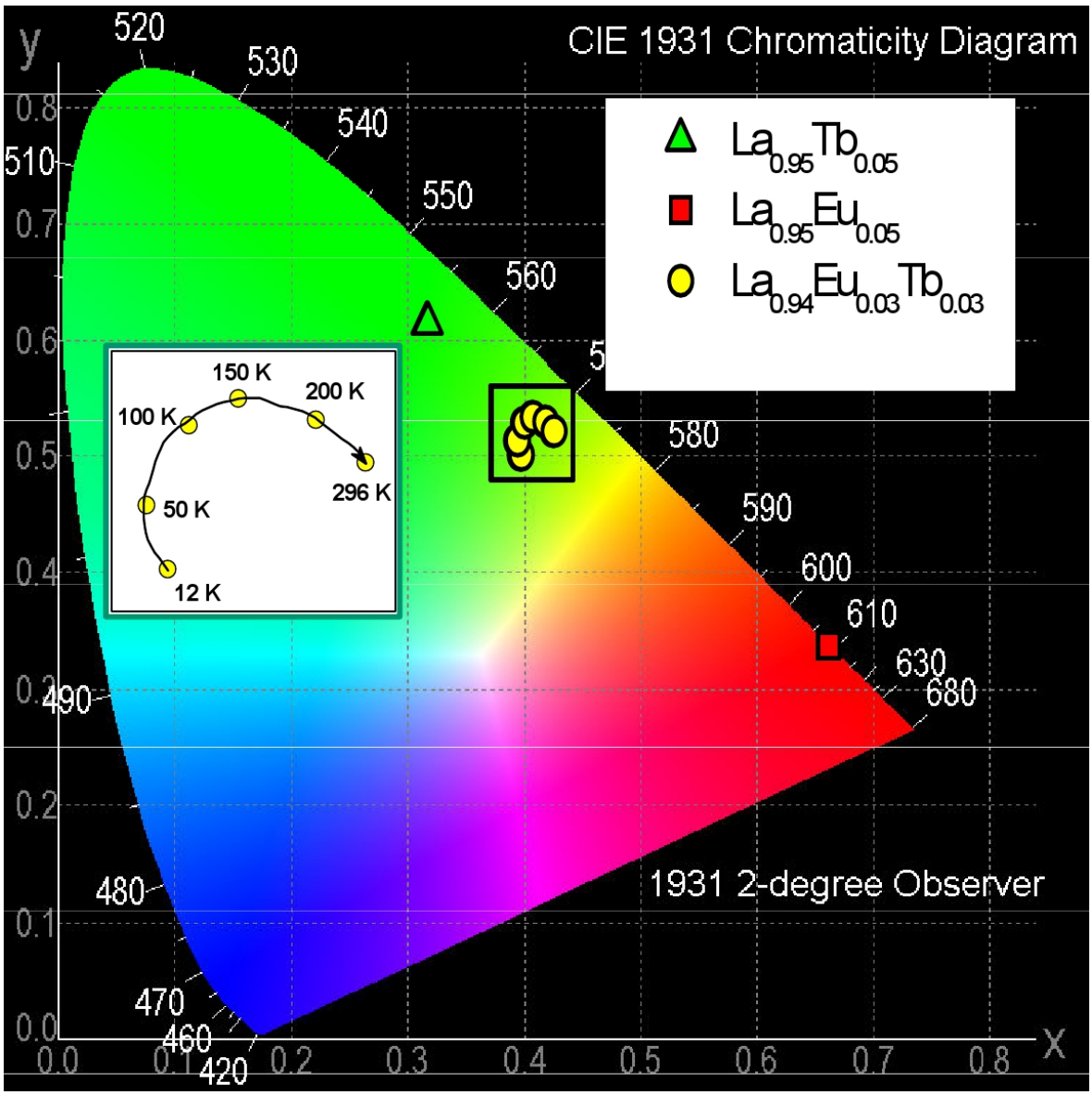

Fig. S29 CIE chromaticity diagram showing the location of the red, green and light green emission at ambient temperature from the $[(La_{0.95}Eu_{0.05})(H_3tftp)(H_2O)]$ (**2**), $[(La_{0.95}Tb_{0.05})(H_3tftp)(H_2O)]$ (**3**) and $[(La_{0.94}Eu_{0.03}Tb_{0.03})(H_3tftp)(H_2O)]$ (**4**) materials, respectively, under 265 nm excitation. The inset shows a magnification of the CIE emission coordinates modifications observed for the mixed Eu^{3+}/Tb^{3+} sample **4** at distinct temperatures.

8. References

1. (a) G. M. Sheldrick, *SHELXS-97, Program for Crystal Structure Solution, University of Göttingen*, 1997; (b) G. M. Sheldrick, *Acta Cryst. A*, 2008, **64**, 112-122.

2. G. M. Sheldrick, *SHELXL-97, Program for Crystal Structure Refinement, University of Göttingen*, 1997.